Skin hydration - How water and osmolytes influence biophysical properties of stratum corneum

Björklund, Sebastian

2013

Skin hydration

How water and osmolytes influence biophysical properties of stratum corneum

Sebastian Björklund

Physical Chemistry

LUND
UNIVERSITY

DOCTORAL THESIS IN PHYSICAL CHEMISTRY

The thesis will, due permission of the Faculty of Science at Lund University, be publicly defended at 10.15 on Friday 14th of June 2013 in lecture hall B, Center for Chemistry and Chemical Engineering, Lund.

The faculty opponent is Professor Jenifer Thewalt,
Department of Physics, Simon Fraser University, Vancouver, Canada

Front cover: Artistic interpretation of the connection, in the form of condensed water drops on spider threads, between the external environment (cloudy sky) and the state of matter (clay ground). Arid conditions with low humidity lead to dehydration and cracking of the clay ground. In a similar manner, changes of the external relative humidity affect the properties of the outermost skin layer. Photos by Hampus Alexander Björklund (hampusalexander.com).

Supervisor:	Emma Sparr, Professor Physical Chemistry, Lund University
Co-supervisors:	Johan Engblom, Associate Professor Biomedical Sciences, Malmö University
	Krister Thuresson, PhD Delta of Sweden, Halmstad, Sweden
Examination board:	Ola Bergendorff, Associate professor Dermatology and Venereology, Lund University
	Katarina Ekelund, PhD LeoPharma, Copenhagen, Denmark
	Luis Bagatolli, Professor Physics, Chemistry, and Pharmacy (MEMPHYS) University of Southern Denmark

Physical Chemistry
Lund University

ISBN 978-91-7422-325-5

Printed in Sweden by Media-Tryck, Lund University
Lund 2013

Organization: Physical Chemistry Center for Chemistry and Chemical Engineering Lund University, P.O. Box 124 SS-221 00 Lund, Sweden	Document name: Doctoral dissertation
	Date of issue: June 14, 2013
	Sponsoring organization: Research school in pharmaceutical sciences (FLÄK).
Author: Sebastian Björklund	

Title and subtitle: Skin hydration – How water and osmolytes influence biophysical properties of stratum corneum

Abstract: The outermost layer of skin (i.e., the stratum corneum, SC) is the interface that separates the water-rich inside of the body from the relatively dry external environment. SC forms an effective permeability barrier, which has to be overcome in transdermal drug delivery. Its function as a barrier for molecular diffusion depends on the SC molecular structure and phase behavior. Both structure and phase behavior may be altered, for example, by hydration or addition of other solutes, which affects the barrier properties.

This thesis explores the interplay between molecular properties of SC components and the macroscopic properties of the SC membrane. We investigate the influence of hydration on SC permeability at steady state by using an *in vitro* set-up where the boundary conditions are controlled by the water activity in the solutions in contact with the skin membrane. Changes of macroscopic properties are rationalized by employing techniques that provide information on SC molecular organization and molecular dynamics.

We show that SC hydration leads to increased SC permeability, which is attributed to a higher fraction of fluid SC molecular components with lower diffusional resistance. This can have implications, for example, in transdermal delivery applications where it is desirable to increase the amount of drug delivered across the skin barrier to reach therapeutic effect.

We show that common so-called moisturizers, like glycerol and urea, can be used to retain high SC permeability under dehydrating conditions. This effect is ascribed to the capability of these small polar molecules to maintain the SC molecular properties in a state that is similar to a more hydrated SC membrane at reduced hydration conditions. This result provides a deeper understanding of the beneficial effect of moisturizers in treatment of dry skin conditions and challenges the view that moisturizers, like glycerol and urea, are beneficial for skin health by merely increasing the SC hydration.

Key words: Stratum corneum, diffusive transport, permeability, flow-through cell, Franz cell, transdermal drug delivery, water activity, vapor pressure, osmotic gradient, relative humidity, ceramide, free fatty acid, cholesterol, keratin filaments, natural moisturizing factor (NMF), urea, glycerol, molecular mobility, ^{13}C natural-abundance solid-state NMR, polarization transfer, isothermal calorimetry, impedance spectroscopy, X-ray diffraction.

Classification system and/or index terms (if any):

Supplementary bibliographical information:		Language: English
ISSN and key title:		ISBN: 978-91-7422-325-5
Recipient's notes:	Number of pages: 188	Price:
	Security classification:	

Contents

Abbreviations ii
List of papers iii
Author contributions iv
Populärvetenskaplig sammanfattning v

1 Introduction 1
The skin 2
Formation, structure, and molecular composition of SC 2
SC as a barrier for molecular diffusion 6
A note on transdermal and topical drug delivery 6
SC is a heterogeneous membrane 8
The scientific questions in this thesis and their relevance 10

2 Experimental techniques and considerations 11
Skin model 11
Measuring water activity with an isothermal calorimeter 12
Steady state flux experiments 14
Polarization transfer solid-state NMR (PT ssNMR) 15
Impedance spectroscopy 17
X-ray diffraction 19
Dynamic vapor sorption microbalance 19
Isothermal sorption calorimetry 20

3 Interplay between hydration and skin permeability 21
A water gradient can be used to regulate drug transport across skin 21
Skin impedance under the influence of a varying water gradient 23
Hydration influences the dynamics of SC molecular components 24
The effect of hydration on the SC structure 27
Molecular insight into the changes of SC permeability upon (de)hydration 29

4 Influence of osmolytes on SC in reduced hydration conditions 31
Glycerol and urea increase skin permeability in reduced hydration conditions 31
The effect of natural moisturizers on SC molecular organization and dynamics 34
Molecular insight into the influence of glycerol and urea on the SC permeability 38

5 Outlook 39

6 Acknowledgements 41

7 References 42

Abbreviations

CP	Cross polarization
CER	Ceramide
Chol	Cholesterol
CSA	Chemical shift anisotropy
DP	Direct polarization
DVS	Dynamic vapor sorption
EM	Electron microscopy
FID	Free induction decay
INEPT	Insensitive nuclei enhanced by polarization transfer
MAS	Magic angle spinning
MeSA	Methyl salicylate
Mz	Metronidazole
NMF	Natural moisturizing factor
NMR	Nuclear magnetic resonance
PBS	Phosphate buffered saline
PT ssNMR	Polarization transfer solid-state nuclear magnetic resonance
PCA	Pyrrolidone carboxylic acid
RF	Radio frequency
RH	Relative humidity
SAXD	Small-angle X-ray diffraction
SC	Stratum corneum
UCA	Urocanic acid
WAXD	Wide-angle X-ray diffraction

List of papers

This thesis is based on the work presented in the following appended papers.

I. **A water gradient can be used to regulate drug transport across skin**
Sebastian Björklund, Johan Engblom, Krister Thuresson, and Emma Sparr
Journal of Controlled Release, 2010, 143, 191-200

II. **Characterization of stratum corneum molecular dynamics by natural-abundance ^{13}C solid-state NMR**
Sebastian Björklund*, Agnieszka Nowacka*, Joke A. Bouwstra, Emma Sparr, and Daniel Topgaard
*These authors contributed equally
PLoS ONE, 2013, 8, e61889

III. **Skin membrane electrical impedance properties under the influence of a varying water gradient**
Sebastian Björklund, Tautgirdaz Ruzgas, Agnieszka Nowacka, Ihab Dahi, Daniel Topgaard, Emma Sparr, and Johan Engblom
Biophysical Journal, *in press*.

IV. **Glycerol and urea can be used to increase skin permeability in reduced hydration conditions**
Sebastian Björklund, Johan Engblom, Krister Thuresson, and Emma Sparr
European Journal of Pharmaceutical Sciences, *in press*.

V. **Stratum corneum molecular mobility in the presence of osmolytes**
Sebastian Björklund, Jenny Andersson, Agnieszka Nowacka, Quoc Dat Pham, Daniel Topgaard, and Emma Sparr
Manuscript

VI. **A calorimetric method to determine water activity**
Sebastian Björklund and Lars Wadsö
Review of Scientific Instruments, 2011, 82, 114903-1

Author contributions

I. I, JE, KT, and ES designed the study. I performed all experiments and analyzed the data. I wrote the paper with contributions from JE, KT, and ES.

II. I, AN, ES and DT designed the study and analyzed the data. I prepared all samples, except the model lipid mixture. AN performed NMR experiments. I and DT wrote the paper with contributions from AN, JAB, and ES.

III. I was responsible for designing the study with input from TR, ES, and JE. I performed impedance experiments with contributions from ID and TR. I and JE performed X-ray diffraction experiments. AN performed NMR experiments. I and TR analyzed the impedance data. I, ES, and JE analyzed the X-ray diffraction data. I and DT analyzed the NMR data. I wrote the paper with contributions from TR, DT, ES, and JE.

IV. I, JE, KT, and ES designed the study. I performed all experiments and analyzed the data. I wrote the paper with contributions from JE, KT, and ES.

V. I, ES, AN, and DT designed the study. I, JA, and QDP prepared the samples. JA, AN, QDP performed NMR experiments. I, JA, AN, DT, and ES analyzed the data. I wrote the manuscript with contributions from JA, DT and ES.

VI. LW designed the experimental set-up. I contributed to the development of the methodology. I performed all measurements. I and LW analyzed the data. LW wrote the first draft of the manuscript, while I prepared the final article with contributions from LW.

Populärvetenskaplig sammanfattning

Hudens fuktighet kan påverkas av många faktorer så som torr luft, ett varmt bad, användning av diskhandskar eller plåster, osv. Men hur påverkas hudbarriären av förändringarna av de yttre förhållandena? Frågan är särskilt relevant i situationer då läkemedel läggs på huden eftersom detta, i de flesta fall, för med sig en förändring av de yttre villkoren som kan påverka barriärens egenskaper.

I denna avhandling undersöker vi samspelet mellan omställningar i den yttre miljön och förändringar av hudbarriärens egenskaper. Huvudsakligen fokuserar vi på vad som händer med barriäregenskaperna när omgivningen förändras från torra till blöta förhållanden. För att definiera vad som menas med torrt eller blött använder vi oss av termen vattenaktivitet, vilken mäts på en skala från 0 (helt torrt) till 1 (rent vatten, dvs. blött). Mer specifikt har vi studerat läkemedelstransport över hudbarriären och hur transport av olika läkemedel beror på omgivningens vattenaktivitet. Vi har även utforskat hur närvaro av små molekyler så som urea och glycerol påverkar läkemedelstransport över huden när omgivningens vattenaktivitet ändras. Dessa substanser är relevanta eftersom de finns naturligt i hudbarriären och även som komponenter i vanliga hudkrämer.

Att få in läkemedel i kroppen via huden är attraktivt, bland annat därför att nedbrytning av den aktiva substansen i detta fall är lägre jämfört med till exempel transport via mag- och tarmkanalen. Trots detta finns det få läkemedel som utnyttjar denna transportväg och förklaringen ligger i att huden utgör en nästan ogenomtränglig barriär mot transport av läkemedel och andra molekyler.

Hudbarriären försäkrar att vi har goda förutsättningar att upprätthålla vår vattenbalans och skyddar mot att farliga kemikalier ska nå kroppen. Barriären finns i den yttersta delen av överhuden som kallas hornlagret (eng. stratum corneum). Hornlagret är ungefär 10 gånger tunnare än ett vanligt pappersark vilket leder till frågan: Hur kan ett så tunt membran utgöra en nästan ogenomsläpplig barriär?

Svaret ligger i hornlagrets uppbyggnad som kan liknas vid en tegelvägg. Tegelstenarna motsvarar döda celler som innehåller hornämne (keratin, trådbildande proteiner) och omges av fettmolekyler som motsvarar det sammanhängande murbruket. Vi fortsätter vår liknelse och tänker oss att en vattenmolekyl eller ett läkemedel ska färdas mellan marken och taknocken av en tegelfasad. Detta innebär att molekylen måste transporteras genom murbruket, men kan i princip undvika tegelstenarna genom att snirkla sig fram genom murbruket. Rådande hypotes är att den kontinuerliga fettfasen, bestående av ordnade och fasta fettmolekyler, till största del ansvarar för hudens barriär. Men vad händer med hornlagrets protein- och fettmolekyler när omgivningens

vattenaktivitet förändras och hur påverkar det transport av olika molekyler genom barriären?

I tre artiklar behandlar vi denna fråga utifrån olika perspektiv. Vi visar att man kan reglera hudbarriärens genomsläpplighet för läkemedel genom att justera vattenaktiviteten i omgivningen; en blöt omgivning leder till ökad läkemedelstransport och vice versa. Vi bidrar till ökad förståelse av de underliggande molekylära förändringarna av hudbarriären, som ytterst avgör barriärens genomsläpplighet för läkemedel. Med experiment baserade på kärnmagnetisk resonans (NMR) har vi kartlagt de dynamiska egenskaperna hos hornlagrets protein- och fettkomponenter. Med hjälp av röntgendiffraktion har vi fått en bild av hur den molekylära strukturen påverkas. Sammantaget visar vi att hornlagrets struktur är relativt opåverkad av omgivningens vattenaktivitet. Däremot påverkas andelen rörliga protein- och fettmolekyler när omgivningens vattenaktivitet förändras; en blöt omgivning leder till fler rörliga molekyler med högre genomsläpplighet och vice versa. Våra resultat bidrar till en molekylär förklaring till varför hudbarriären är mer genomsläpplig när omgivningen är blöt och omvänt mindre genomsläpplig i en torrare miljö. I praktiken kan resultaten ha konsekvenser för hur man väljer att utforma läkemedelsformuleringar avsedda för att antingen nå det systemiska blodomloppet eller i situationer när man vill behandla huden lokalt och eventuellt minimera transporten genom hornlagret.

I två artiklar visar vi att urea och glycerol kan användas för att öka hudbarriärens genomsläpplighet för läkemedel vid låga vattenaktiviteter. En relativt torr omgivning med närvaro av urea eller glycerol leder till likartat högt läkemedelsflöde över barriären som när omgivningen är blöt. Detta resultat kan relateras till att glycerol och urea bevarar hornlagrets struktur vid lägre vattenaktiviteter, sett utifrån röntgendiffraktion. Vi visar även att glycerol och urea kan bibehålla samma dynamiska egenskaper av protein- och lipidkomponenterna vid torra förhållanden som samma komponenter har vid fuktiga förhållanden. En viktig slutsats är att glycerol och urea kan användas för att öka hudbarriärens genomsläpplighet i torra förhållanden där vatten avdunstar medan dessa molekyler inte gör så. Studierna belyser även en annan viktig aspekt, nämligen att glycerol och urea inte nödvändigtvis ökar hudens fuktighet utan snarare bevarar den fuktiga hudbarriärens dynamiska egenskaper i torra förhållanden.

Slutligen har vi utvecklat en mätmetod för att bestämma vattenaktiviteten i lösningar eller fasta material vilken vi visar vara särskilt känslig för höga vattenaktiviteter där mer konventionella metoder tappar sin säkerhet. Metoden har använts för att fastställa vattenaktiviteten i våra olika läkemedelsformuleringar och ytterst säkerställa att vi har väldefinierade förhållanden med avseende på vattenaktiviteten i våra studier av läkemedelstransport över hudbarriären.

1 Introduction

The water balance of our body is crucial for homeostasis and because water is the main component of our body it is vital that the body has an excellent barrier to prevent dehydration. The barrier that protects us from desiccation is provided by our skin, which is the interface between the internal body and the external surroundings. The skin barrier properties are not static, but rather responsive to changes of the external environment, such as temperature or relative humidity. Prosaic examples of responsive interplay between barrier properties and variation of external parameters are dry skin features, common to habitants in cold and dry climate, or wrinkly skin after a long bath. From a scientific perspective, it is relevant to understand how and why the skin barrier is affected by changes of the surrounding conditions. This understanding has implications with respect to, for example, uptake of drugs applied on the skin surface, how skin disorders progress, and skin health in general.

The interplay between the external environment and the properties of the skin barrier is the focus of this thesis. In particular, the objective is to systematically investigate how macroscopic properties of the skin barrier, such as its permeability, are affected by its degree of hydration. To fully appreciate this interplay it is necessary to obtain molecular scale information on the structure and dynamics of the components making up the skin barrier, which is also accomplished in this work.

This chapter gives an introduction to the skin barrier and outlines the relevance of the scientific questions posed in papers I-VI. Chapter 2 gives an account on the experimental techniques used in this work and some experimental considerations. Chapter 3 focuses on the relationship between skin permeability and skin electrical impedance properties under the influence of varying hydration conditions. The understanding of this relationship is rationalized by using techniques that provide information on the molecular structure and dynamics of the skin barrier components. In chapter 4 the influence of hydration on the skin permeability is further investigated for situations where naturally occurring osmolytes are present; a situation that is shown to affect the outcome both on a macroscopic and molecular scale. Finally, chapter 5 presents an outlook for future research related to this thesis work.

The skin

The average skin surface area of an adult is around 1.7 m^2 (1, 2). This is a large area of exposure considering that one of the main functions of the skin is to act as a permeability barrier by preventing water loss and entrance of harmful substances. The skin also accommodate many other important functions, such as providing a defense system for microbial pathogens, insulation and thermal regulation, and a general protection against injuries (3, 4). The skin provides these functions under constant exposure of mechanical stress as body parts bend and stretch, which requires a strong and elastic skin tissue. These mentioned functions are connected to different anatomical entities of the skin, which in general is divided into following different regions; hypodermis (subcutis), dermis, and epidermis. The epidermis may, in turn, be divided into the viable epidermis and the stratum corneum (SC). SC is the most relevant region for this work as it represents the main permeability barrier (5). The excellent barrier properties of SC are connected to its molecular composition and structure.

Formation, structure, and molecular composition of SC

The skin is a dynamic organ undergoing constant biosynthesis and regeneration of new tissue at the same rate as old tissue is discarded from the skin surface. These processes are intimately linked under homeostatic control and involves a multitude of steps, such as cell division, migration, maturation, terminal differentiation, lipid metabolism, and breakdown of structures responsible for cell cohesion to allow for removal of old tissue (i.e. desquamation) (4). A detailed description of these and other processes underlying the formation of an intact SC is not given here. Instead, Figure 1.1 suffices as a simple representation of the epidermis and captures some relevant features of the various stages of the SC formation (4, 6-8). Epidermal stem cells (keratinocytes) are attached to the basal layer by hemidesmosomes. Upon biochemical activation, the keratinocytes detach from the basal membrane and start to migrate through the spinous and granular layers. During this process the expression of keratin proteins K1 and K10 is initiated and the keratinocytes lose their columnar shape and become more flat (7). In the spinous and granular regions, the keratinocytes are joined together by structural proteins referred to as desmosomes (4). A cornified cell envelope is developed in the upper spinous region, which consists of a macromolecular assembly of cross-linked proteins (7). When reaching SC, the cells are terminally differentiated into flat

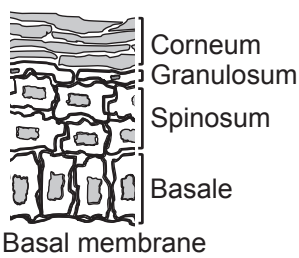

FIGURE 1.1. Stratified layers of the epidermis.

hexagonal-shaped disks of approximately 0.3 μm thickness and 30 μm in diameter (8). In the SC, the cells are referred to as corneocytes, which are joined together by modified desmosomes (called corneodesmosomes) (4). The transition from stratum granulosum to SC also involves secretion of lipid material, derived from the intracellular organelles and cell nucleus, and important metabolic activity to form the lipids of the extracellular matrix (4).

The structure of SC can be resembled with that of a brick wall (Figure 1.2) with the corneocytes represented as bricks and the extracellular lipids represented by the continuous mortar (9, 10). Typically, the SC comprises 10-30 cell layers, which correspond to a thickness of around 5-20 μm (8). As discussed in more detail below, the SC is not as homogeneous as the schematic structure in Figure 1.2.

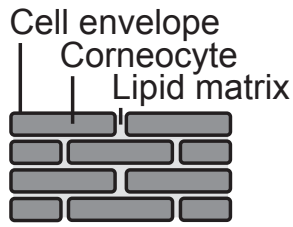

FIGURE 1.2. Bricks and mortar representation of the SC.

Mortar

The lipid material mainly consists of ceramides, free fatty acids, and cholesterol in a relatively equal molar ratio, together with a minor fraction of cholesterol sulfate and cholesteryl esters (11). The chemical structure of relevant SC lipids, employed in paper II, is given in Figure 1.3 where ceramide names are according to reference (12).

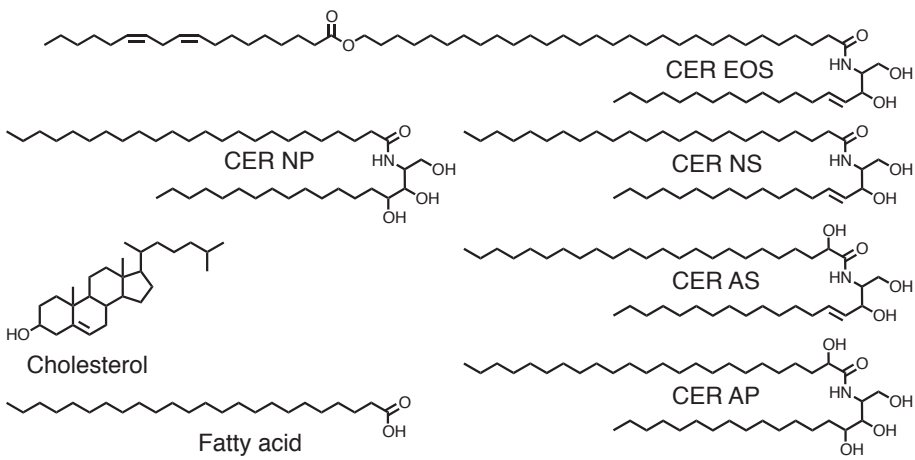

FIGURE 1.3. Representative lipid species in SC. Ceramide (CER) nomenclature: S and P is for sphingosine and phytosphingosine, respectively, O stands for ω-OH fatty acid, N represents a normal fatty acid, and A is for α-OH fatty acid, while E represents an ester-linked fatty acid.

In addition to the continuous lipid matrix, the cornified cell envelope has a covalently bound lipid layer facing the extracellular region, which is comprised of mainly ceramides, but also fatty acids and ω-hydroxyacid (11). The lipid envelope (LE) is suggested to play an important role for proper formation of the lipid lamellae matrix (13-16). The SC lipids comprise a heterogeneous mixture with varying carbon chain lengths in the range of C14-C32, of which most are saturated (17, 18). Carbon chains with C20/C22 are the most common free fatty acids, while C20 and C24 have highest occurrence of the sphingosine and the amide linked fatty acids, respectively, of the lipids in pig SC (used in this work) (17, 18). Compared to the lipids found in most cellular biomembranes (19), the SC lipids are unusually long and more saturated. These properties favor the formation of crystalline or solid gel structures at normal skin temperatures (ca. 28-32 °C). Indeed, several studies have shown that the main fraction of the lipid lamellae in intact SC are in a solid state, while lipids in a more fluid state represents a minor portion (20-28).

Based on electron microscopy and X-ray diffraction methods, together with knowledge of the lipid composition, several models of the molecular organization of the SC lipid lamellae have been proposed (28-31). The main conclusion from these investigations, and the proposed models, is that the SC lipids form lamellar structures with a repeat distance of around 11-13 nm and predominantly orthorhombic packing of the acyl chains in human SC, and hexagonal acyl chain packing in pig SC (32).

For illustrative purposes, Figure 1.4 shows one repeat unit of the trilamellae model proposed by Hill and Wertz (2003), where each lamella is around 4.2 nm in thickness. The structure is located in between two facing lipid envelopes (LE) (13-15, 31). According to this model the unsaturated linoleate acyl chains are located in the central lamella, which is suggested to result in a more fluid-like packing of the carbon chains in this region. This arrangement is similar to the model suggested by Bouwstra et al. (29). More recently, Norlen et al. (2012) put forward a model where the ceramide carbon chains (i.e. the sphingosine and fatty acid chains) are configurated antiparallel to each other, with cholesterol preferentially associated with the sphingosine acyl chains (28).

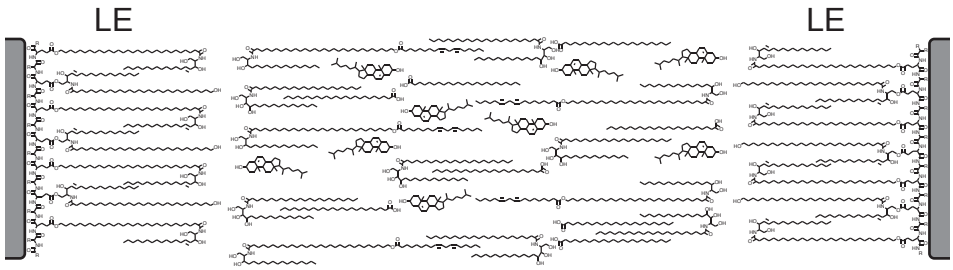

FIGURE 1.4. One of several molecular models of SC lipid organization. This model was proposed by Hill and Wertz (2003) and consists of a 12.9 nm trilamellar structure (i.e. three 4.3 nm lamella), visualized here in between the lipid envelopes (LE) of two adjacent corneocytes. Here, LE is represented by covalently bound CER OS, while the extracellular lipids are illustrated by cholesterol, fatty acid, CER EOS, and CER NP.

Bricks

Approximately 85wt% of the dry SC tissue consists of proteins, which is mainly ascribed to the corneocytes (4). The intracellular regions of the corneocytes contain primarily keratin filaments. Figure 1.5 shows the hierarchical organization of the keratin filaments, schematically envisaged as rods (7, 33, 34). One filament consists of bundles of eight protofilaments, each with a diameter of 2-3 nm, resulting in a total diameter of 8-10 nm. The protofilaments are made up of end-to-end aggregated tetramers, which in turn are comprised of two coiled-coil heterodimers associated in an antiparallel and staggered configuration. The heterodimers consists of pairs of keratin monomers, of which one is acidic (type I) and one is neutral-basic (type II), associated together in a parallel arrangement. The length of coiled-coil dimers is approximately 50 nm. Characteristic for the keratin monomers is the central α-helical rod domain with relatively high configurational order, which is flanked by two more disordered N- and C-terminal domains. The latter domains have high glycine and serine contents in the particular case of keratin monomers K1 (type II) and K10 (type I), which are predominantly expressed in SC and upper epidermis.

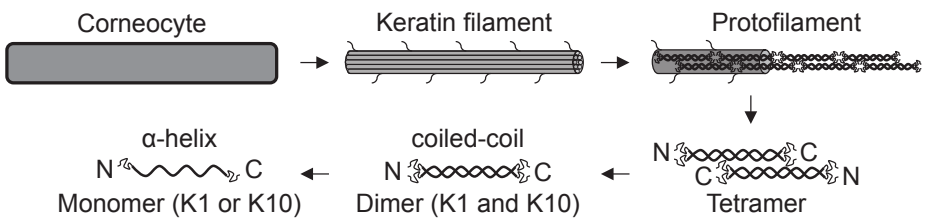

FIGURE 1.5. Structural hierarchy of keratin filaments.

SC as a barrier for molecular diffusion

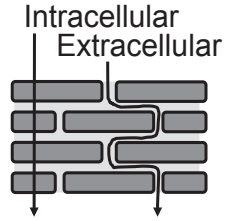

FIGURE 1.6. Transepidermal pathways of molecular diffusion through SC.

The potential pathways for a molecule to diffuse through the skin barrier are via the transepidermal route or via the appendages (sweat glands, hair follicles, sebaceous glands) (5). The relevance of these different routes in various applications is still a subject for discussion. The route through or via the appendages is generally suggested to be of minor importance as the total surface of these structures is limited (estimated to 0.1 % of the total skin surface area) (5). Recently, this view has been questioned based on studies showing that the hair follicles can contribute to the penetration of topically applied drugs (35). The magnitude of this contribution depends on the body site and the type of drug substance applied (35).

Transepidermal diffusional transport can occur via the intracellular and the extracellular regions (Figure 1.6), of which the latter presents a continuous pathway through the SC. In other words, for transepidermal transport of a molecule across SC it has to pass the extracellular lipid matrix, while the intracellular regions in principle can be avoided. Thus, without excluding any of these two routes it is clear that the extracellular lipid domains will in all cases influence the diffusional properties of molecules. In the literature, the extracellular path is largely considered to be most relevant for diffusional transport across the skin barrier (36-40). This route of molecular transport involves diffusion and partitioning into both the relatively hydrophilic headgroup regions and the hydrophobic interior of the hydrocarbon chains of the multilamellar lipid structures. In relation to this it is clear that the high fraction of SC lipids in the solid state can assure low permeability. The presence of fluid lipids (26, 27, 32) can, however, have large consequences for the permeability by potentially forming regions with lower diffusional resistance where transport preferentially occurs (30).

A note on transdermal and topical drug delivery

The structural properties of SC represent an exceptional barrier for molecular transport both in and out from the body. Despite this, transdermal delivery of drugs is an attractive alternative to the oral route. One reason being that it is associated with lower degree of first pass metabolism, whereby the concentration of the drug is reduced before it reaches the systemic circulation. It is evident that only certain molecules with appropriate physicochemical properties are relevant for consideration of transdermal delivery by passive diffusional transport. For example, the molecular weight (MW) of the active drug should preferably be less than 500

Da and the octanol-water partition coefficient (log $K_{o/w}$) should be around 1-3 (41). The first transdermal product for systemic delivery was a patch for treatment of motion sickness with the active ingredient scopolamine (MW=303 Da, log $K_{o/w}$=1.24), which was approved in 1979 in the US (41, 42). About a decade later a patch containing nicotine (MW=162 Da, log $K_{o/w}$=1.17) became a great success (41, 42). Since then several strategies to overcome the SC transport barrier have been developed, such as iontophoresis (43), electroporation (44), microneedles (45), ultrasound-mediated techniques (46), and penetration enhancers (47). Despite much effort, there is still only about 40 products with around 20 different active drugs on the market, of which most are based on transdermal patches (42, 48).

Topical medication usually refers to local treatment of, for example, various skin diseases or local pain relief, both cases involving an active ingredient. A clear advantage of, for example, using a topical application for local pain relief is that the systemic effect, and unwanted effects on the stomach and intestine in the case of oral delivery of pain-relieving pills, is avoided. If one includes ordinary creams, lotions, ointments, and gels, used for more daily treatment of skin, to the topical medication compartment, it is undoubtedly a large industry. The model drugs used in this work are two examples of ingredients in topical formulations. Metronidazole (MW=171 Da, log $K_{o/w}$=-0.02) is an antibacterial drug used for treatment of the skin disease rosacea, while methyl salicylate (MW=152, log $K_{o/w}$=2.48) is commonly used in liniments (49, 50).

SC is a heterogeneous membrane

It is obvious that SC is a heterogeneous membrane with local variations in the molecular composition and structural properties. For example, the number of corneodesmosomes is lower in the upper SC regions compared to the lower regions (51) and the lipid composition varies at different positions in SC (52-55). These differences are often related to altered functional properties and may be connected to the continuous maturation of SC and the final desquamation process (4). The observed drop in cholesterol sulfate in the outer SC region is suggested to destabilize the lipid lamellar structures, which may work in conjuncture with the lower number of corneodesmosomes to allow easier detachment of corneocytes from the SC surface (54-56). There are also gradients in the concentration of various salt ions (57) and the pH (58) between the inner and outer regions of SC. The pH dependence of protease activity is suggested to play a role during desquamation (59), while potassium and calcium ions have been shown to influence the ability of SC to recover after acetone exposure (60).

The water gradient across SC and the presence of osmolytes

Hydration of SC is of particular importance in this work. At normal conditions the water content is around 70wt% in the viable epidermis and around 20wt% in the outermost SC, with a steep change between the corneum and granular layers (61, 62). From this profile in water content we cannot determine the local water activity in the different SC regions, as this is dependent on both molecular composition and structural properties. As discussed above, SC is a heterogeneous membrane with local variation in molecular composition and structure. We can, however, conclude that the water activity in the viable epidermis is controlled at physiological conditions, while the water activity of the external environment in most cases is lower as compared to the water-rich viable tissue. As a consequence, there is a gradient in water activity across SC to the external environment, which leads to continuous transport of water by passive diffusion. This process is referred to as transepidermal water loss (TEWL) and provides the SC with water.

Historically, SC hydration has been viewed as vital for maintaining cohesion and flexibility of the cornified tissue in the skin barrier (63), while more recent research has emphasized the importance of sufficient amount of water for biochemical reactions to take place (64-67). Interestingly, there seems to be a well-regulated interplay between the SC water content, enzyme activity, filaggrin degradation, and production of small polar osmolytes (64, 65). There is an inverse correlation between the water content profile of the SC and several osmolytes, such as free amino acids and their derivatives (68). The osmolytes are derived from different sources, of which the filaggrin hydrolysis into amino acids represents a major one.

Following filaggrin degradation, the amino acids may be further metabolized into derivatives such as pyrrolidone carboxylic acid (PCA) by non-enzymic cyclization of glutamine (69) and urocanic acid (UCA) by conversion of histidine by histidase (70). Other sources are introduction of osmolytes from sweat (e.g. urea), via epidermal circulation, or from triglyceride turnover in sebaceous glands (e.g. glycerol) (68, 71). Considering these different sources, the osmolytes may be distributed in various regions of the SC, but it can be expected that the osmolytes are predominantly present in the aqueous regions of SC due to their polar characteristics.

What are osmolytes and why are they present in SC?

In general, the presence of small water-soluble substances in relatively high concentrations is a common property for organisms exposed to osmotic stress in nature (72). One function of these molecules is to prevent osmotic stress of cells or other tissues by balancing the osmotic pressure of the external environment, while maintaining vitality of the cells or tissues. In contrast to elevated concentrations of electrolytes, the osmolytes do not generally compromise the function and structure of the living system (72). However, these molecules are not completely interchangeable as they may act differently on different biological systems and be associated with more complex biological processes than simply regulate the osmotic pressure (73). As already stated, the SC is particularly exposed to osmotic stress from dry and cold climate of the external environment. Therefore, it is not surprising that this type of small polar molecules is naturally present in SC. In the field of skin cosmetics and dermatology the osmolytes are referred to as the natural moisturizing factor (NMF), and these components are known to be beneficial for skin suffering from dry conditions (74). Several studies have also demonstrated that various skin diseases are associated with reduced levels of these molecules (75, 76).

The scientific questions in this thesis and their relevance

In this work, we will consider alterations of the SC structure as a response to variations of external parameters, such as the water activity or the introduction of osmolytes. These changes occur on relatively short time scales and primarily involve alterations of the SC molecular phase properties, which can influence the macroscopic behavior. This time scale may differ from the biochemical changes of SC, such as desquamation and generation of NMF components, which take place over relatively long periods in an intricate and continuous manner.

The influence of hydration on skin permeability is particularly relevant for transdermal or topical drug delivery applications because, in most cases, the degree of SC hydration is altered at the area of application. In general, it is known that changed skin hydration can affect the skin permeability and this is taken advantage of in some cases. For example, occluding the skin surface with an impermeable dressing on the drug application site leads to elevated hydration and in most cases increased skin permeability (77, 78). The details of how skin hydration influences the permeability, structure, and molecular properties of SC are, however, not resolved. Why does the skin, in most cases, become more permeable for both hydrophilic and hydrophobic molecules when SC contains more (polar) water? Is there a threshold hydration level of SC that must be met for the skin barrier to become more permeable? How does hydration affect the structure and mobility of the SC molecular lipid and protein components? Papers I-III systematically explore these questions by combining studies on the skin permeability to model drugs and characterization of SC at different levels of hydrations by means of impedance spectroscopy, X-ray diffraction, and solid-state NMR methods.

In general, the NMF components are described to be beneficial for dry skin due to their capability of increasing SC hydration under dry conditions (68, 74). Why is this beneficial? Is it because the NMF components increase the SC water content, which in turn can alter the physical state of the SC components (79-82)? Interestingly, it has been demonstrated that small polar molecules (other than water), such as NMF, have a strong influence on the phase behavior of model lipid systems in dry conditions, where they act to retain lipid fluidity (83, 84). Is this mechanism relevant for SC or does it depend on the water content alone? We hypothesized that a similar mechanism of retained fluidity of molecular matter is important in situations where osmolytes are present in SC under dehydrating conditions. If osmolytes act to retain fluidity of the SC components, this would likely also influence the SC permeability. In papers IV and V, we investigate how the SC permeability, and the molecular structure and dynamics of SC components, is influenced by hydration, in the presence of glycerol, urea, PCA, and UCA. These studies aim at providing a more detailed picture of how osmolytes and the NMF components influence the SC properties.

2 Experimental techniques and considerations

This section gives a brief account on some of the experimental techniques used in this thesis work, and it describes some experimental considerations. A description of standard methods employed in this work, such as UV-spectroscopy or reversed-phase high-pressure liquid chromatography (paper I and IV), and protocols for determining model drug solubility (paper I and IV) or extraction of SC lipids (paper II and V), is not given in this summary.

Skin model

Pig skin was used in this work, as it represents a relevant model to human skin in terms of anatomy (85), lipid composition (18), permeability (86-90), and electrical properties (90, 91). Dermatomed skin membranes, ~ 500 μm in thickness, consisting of SC, viable epidermis, and parts of dermis, were used in the drug permeability studies and impedance spectroscopy experiments. It is widely accepted that the diffusional resistance of molecules and the electrical impedance are mainly associated with the SC layer, while the contribution from the underlying viable tissue is negligible (5, 92-94). For this reason, and because of the practically more demanding task to separate intact SC tissue without any defects, dermatomed skin membranes were used. In the solid-state NMR, X-ray diffraction, and DVS experiments, the SC was separated from the viable epidermis to enable total focus on the most relevant molecular components in terms of barrier properties. These techniques are not sensitive to macroscopic defects and it is thus of minor importance if the SC tissue does not remain macroscopically intact.

SC samples were equilibrated both in aqueous solutions (paper III and IV) and in vapor with controlled RH (paper II, III, and V). In the former case the samples consisted of SC sheets, while pulverized SC was used in the latter case to decrease the preparation time. No differences between these types of samples could be observed. Additional diffraction data (unpublished) are presented in the thesis summary (Table 3.1), and these SC samples were pulverized and prepared in vapor with defined RH according to the same procedure as in paper II and III.

Measuring water activity with an isothermal calorimeter

In papers I, III, and IV we characterize the chemical potential of water $\Delta\mu_w$ in the aqueous drug formulations in terms of the water activity a_w, which is derived from fundamental principles of thermodynamics. At thermodynamic equilibrium $a_w = f/f_0$, where f is the fugacity of water in the system and f_0 is the fugacity of pure water at the corresponding temperature. At ambient constant temperature and atmospheric pressure the water activity is closely approximated by $a_w = p/p_0$, where p is the water vapor pressure above the formulation and p_0 is the saturation vapor pressure of pure water. The chemical potential of water can also be expressed in terms of relative humidity RH or osmotic pressure Π_{osm} with the relation:

$$\Delta\mu_w = RT\ln(a_w) = RT\ln(p/p_0) = RT\ln(\mathrm{RH}/100) = -V_w\Pi_{osm}$$

where V_w is the molar volume of water, R is the gas constant, and T is the absolute temperature. Here it can be noted that in medicine the term osmolarity is often encountered. This term refers to the concentration of salt ions, mainly sodium and chloride, responsible for regulating the osmotic pressure in plasma and serum, which is tightly controlled around 280-290 mosm/l (95) and corresponds to the a_w in a physiological saline buffer ($a_w \sim 0.995$).

Considering the pivotal role of the water activity in this work, it is most relevant to have a reliable method to determine this parameter. In paper I, we used a method based on capacitive RH sensors to determine a_w. The sensors respond to changes in the RH by an alteration in the capacitive properties and after calibration this method provide reliable readings at most RHs. However, in the high RH range (above RH ~ 98%) this method does not provide consistent data, which is a limitation common to most conventional methods employing capacitive, resistive, or chilled mirror sensors. This problem initiated the development of an isothermal calorimetric method to determine a_w, which is detailed in paper VI. A general benefit of using an isothermal heat conduction calorimeter is the strict control of the temperature, which is crucial for precision measurements of a_w, foremost due to that the saturation vapor pressure is dependent on the temperature. For example, a temperature variation of only 0.01 °C leads to almost 1% alteration of the saturation vapor pressure at ambient temperatures (96). A particular advantage of the method is that it relies on the end-points $a_w=0$ and $a_w=1$ as references. Thus, the technique covers the full a_w range and does not require calibration or reference values from the literature.

The method is fundamentally based on the transpiration method described as early as 1845 (97) and follows similar principles as explained by Berling et al. (98, 99). In brief, the method works by letting a dry stream of N_2 gas flow over a solution with unknown a_w under controlled conditions so that equilibrium between a_w in

the sample and the gas is adequately achieved. Once this is fulfilled, the humidified gas is introduced into the calorimetric measuring vessel, which contains pure water. The difference in a_w between the humidified gas and the pure water leads to endothermic evaporation of water and this process is measured in the calorimeter. Next, completely dry gas (a_w equal to 0) is introduced into the measuring cell, still containing pure water, and the endothermic evaporation is recorded and used as a reference. At the end we obtain two measured endothermic outputs, one belonging to the reference with known a_w (equal to 0) and the other related to the unknown a_w in the sample, which now can be determined. This is the working principle, which is detailed in paper VI where the method was evaluated by measuring the a_w in a range of aqueous NaCl solutions and saturated salt solutions. In conclusion, paper VI shows that our method provides experimental data of a_w in good agreement with the literature over the full a_w range and with excellent performance in the high a_w range.

In paper IV we used the calorimetric method to determine the a_w in various model drug formulations containing glycerol or urea. Figure 2.1 shows data on glycerol (G) and urea (U) in PBS solution, with the model drug metronidazole (Mz) present. A comparison with previous experimental data (100) on glycerol (G, lit.) and urea (U, lit.) in pure water show good agreement. In average, our data are 0.007 below the reference data. This shift corresponds to the presence of buffer salts and the model drug, resulting in a difference of 0.008 between PBS with Mz (a_w=0.992) and pure water (a_w=1).

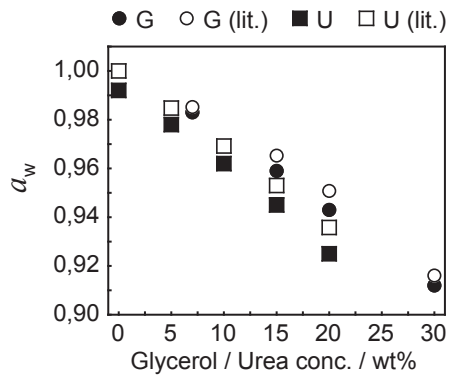

Figure 2.1. Water activity (a_w) as a function of glycerol (G) and urea (U) concentration in PBS solution, also containing the model drug Mz, as determined with the isothermal calorimetric method. Reference data (lit.) from corresponding concentrations of glycerol and urea in pure water is included for comparison (100).

Steady state flux experiments

The skin membrane is a complicated tissue associated with natural variability. Considering this, it is suitable to employ an experimental system with well-defined boundary conditions and simple formulations with a minimal number of components to avoid any additional complexity. This aspect is reflected in the steady state flux methodology used in papers I and IV.

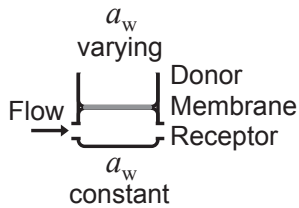

FIGURE 2.2 Flow-through diffusion cell.

Figure 2.2 shows a schematic representation of the flow-through diffusion cell. The water activity in the receptor solution is fixed at physiological conditions, while the water activity in the donor phase is regulated by water-soluble polymers. The size of the flexible polymer is relatively small (1500-4000 Da) to allow for a considerable decrease in the colligative water activity property, still comparatively large to avoid penetration of the polymer into the SC (101-104). In paper IV, glycerol or urea was used in addition to the polymer to regulate the water activity. In all experiments, the influence of the formulation composition with respect to the chemical activity of the model drug was considered by determining the model drug solubility in all formulations. The model drug concentration was then adjusted accordingly, as described in papers I and IV. Control experiments with silicone membranes were performed in all cases to ensure that the steady state flux over the inert silicone membranes was identical for all formulations.

As shown in papers I and IV, this was fulfilled and proves that each formulation have the same release rate irrespective of composition. Thus, any changes in steady state flux observed for the skin membranes cannot be ascribed to differences related to the formulation composition, other than the variation in water activity. To assure steady state conditions, the receptor solution was continuously renewed to avoid build-up of model drug concentration, while the volume of the donor solutions was sufficiently large for concentration changes to be negligible. Under these given conditions, any changes of the steady state flux of the model drug across the skin membrane can be ascribed to alterations of the membrane material properties, such as its structure or phase behavior, which can influence the model drug solubility and diffusion coefficient in different regions of the SC (105).

Polarization transfer solid-state NMR (PT ssNMR)

All nuclei (except one) are made up of protons and neutrons that possess a property called spin. If the sum of spins from an individual nucleus is nonzero the nucleus will behave as a weak magnet when placed in a magnetic field. This property, shared by several nuclei, is a prerequisite in NMR spectroscopy. Common nuclei in NMR studies are ^{1}H and ^{13}C, both having spin-1/2 and a natural abundance of ~ 99% and ~ 1%, respectively.

After allowing the nuclei to equilibrate in the external magnetic field B_0, the spins will, in average, be slightly more aligned in parallel with B_0 than any other direction and thus create a bulk magnetization M. By convention the direction B_0 is along the longitudinal z-axis. The bulk magnetization of the sample can be envisaged as a vector precessing around the direction of B_0 with a frequency defined by the Larmor frequency ω_0. The direction of M can be manipulated by applying a RF pulse with the same frequency as ω_0. The RF pulse introduces a temporary magnetic field B_1 that affects the direction of M and the pulse length regulates the angle with which the pulse flip M relative to the longitudinal axis. The combination of pulses is called a pulse sequence. The return of M into equilibrium is described by longitudinal relaxation and quantified by the relaxation time T_1. Transverse relaxation occurs when M is tilted into the xy-plane and the spins, initially in-phase, become continuously more out-of-phase, which ultimately results in zero transverse magnetization at equilibrium. This process is described by the relaxation time T_2 and is related to the free induction decay (FID) signal, which contains signal contribution from different resonances of the same nucleus.

In pulsed NMR spectroscopy, the FID is recorded over time and Fourier transformed into the frequency domain. By convention an NMR spectrum display signal intensity as a function of chemical shift δ, where δ is obtained by normalizing the frequency in relation to the resonance frequency of a standard molecule at the applied magnetic field. The location of a peak in the spectrum depends on its resonance frequency, which is influenced by the local magnetic field arising from the electron distribution of the atom and the molecular environment in which the nucleus is located.

The natural-abundance ^{13}C NMR methodology used in this work (PT ssNMR) was developed by Nowacka and Topgaard, and this is a powerful tool to characterize the molecular dynamics of self-assembled systems in the low water regime (106, 107). A fundamental aspect of PT ssNMR is that it involves magic angle spinning (MAS) and heteronuclear decoupling to minimize peak broadening from chemical shift anisotropy (CSA) and heteronuclear scalar and dipolar couplings, to obtain ^{13}C segmental resolution in the chemical shift scale (108).

Information on the molecular dynamics is given by comparing the signal intensities acquired in the INEPT and CP pulse sequences, relative to the signal obtained from the DP experiment. INEPT is normally used to enhance the signal in liquid state NMR (109), while CP is a corresponding standard scheme employed in solid-state NMR (110). The DP experiment does not involve polarization transfer and the DP signal intensity may thus be used as a reference in comparison to the INEPT and CP signal intensities. When the DP, INEPT, and CP experiments are applied on the same sample the signal from a specific resolved segment will depend on its dynamical properties, which may be defined in terms of mobility or rigidity. The distinction between rigid and mobile molecular segments is rationalized by the relation between the experimental DP, INEPT, and CP signal intensities with respect to the theoretical signal intensity ratios (106). This comparison has been validated for different self-assembled systems with known phase behavior (84, 106, 107).

Figure 2.3 shows calculated signal intensities for a $^{13}C^{1}H_2$ segment based on the theoretical model, which is detailed in the work of Nowacka and Topgaard (106). The INEPT and CP signal intensities vary as a function of the rotational correlation time τ_c and the ^{13}C-^{1}H bond order parameter S_{CH}, from which it is possible to distinguish different dynamic regimes (cf. Figure 2.3) (106). τ_c measures the rate of the ^{13}C-^{1}H bond reorientations, while S_{CH} quantifies the time-averaged orientation of the ^{13}C-^{1}H bonds with respect to a main symmetry axis (e.g. the normal axis of a lipid bilayer) and is thus a measure of anisotropy.

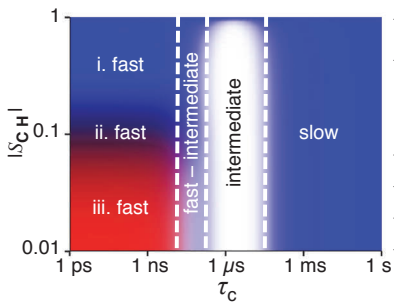

Dynamic regime	τ_C	$\lvert S_{CH}\rvert$	Intensity
i. fast	< 10 ns	< 0.01	INEPT >> CP = 0
ii. fast		≈ 0.1	INEPT = CP
iii. fast		> 0.5	CP >> INEPT = 0
fast-intermediate	≈ 0.1 μs		CP >> INEPT = 0
intermediate	≈ 1 μs		CP = INEPT = 0
slow	> 0.1 ms		CP >> INEPT = 0

FIGURE 2.3. Theoretical INEPT (red) and CP (blue) signal intensities for a $^{13}C^{1}H_2$ segment as a function of C-H bond order parameter S_{CH} and correlation time τ_c in different dynamic regimes under 5 kHz MAS and 11.74 T magnetic field, B_0 (left). White represents inefficient INEPT and CP polarization transfer. The general division of dynamic regimes is based on the tabulated values for τ_c and S_{CH} (right). Adopted from (106).

Both the INEPT and the CP pulse sequences transfer magnetization from ^{1}H nuclei to neighboring ^{13}C. The polarization transfer occurs in different ways, and this is taken advantage of in PT ssNMR for selective signal enhancement of mobile or rigid molecular segments. INEPT transfer magnetization via through-bond scalar couplings, which are not influenced by bond reorientation. A prerequisite for

INEPT signal is that the ^{1}H and ^{13}C transverse relaxation times ($T_2^{H/C}$) are longer than the time required for ^{1}H-^{13}C polarization transfer to occur. $T_2^{H/C}$ is long for mobile segments with isotropic reorientation due to that the time-averaged ^{1}H-^{1}H and ^{1}H-^{13}C dipolar interactions disappear in this case (cf. Figure 2.3, fast regime and case iii). Short $T_2^{H/C}$ results in inefficient INEPT signal for segments in the fast regime with anisotropic reorientation (cf. Figure 2.3, fast regime and case i). CP transfer polarization via through-space dipolar interactions and the time for this process is determined by the cross polarization time constant T_{CH}. T_{CH} is fast for segments in the slow regime and/or segments with anisotropic reorientations, leading to efficient CP signal in this case (cf. Figure 2.3, slow regime or fast regime and case i). The CP efficiency is also dependent on the ^{1}H longitudinal relaxation time in the rotating frame ($T_{1\rho}^{H}$), which in the intermediate regime is too fast for CP to be effective.

Impedance spectroscopy

Impedance spectroscopy is an established technique in electrochemistry that has gained attention in skin research. For example, as a tool for characterizing the effect of transdermal delivery of charged compounds by iontophoresis on the skin membrane (111, 112), and for probing skin hydration (93). Impedance in its simplest form describes the relation between voltage and current over a range of frequencies.

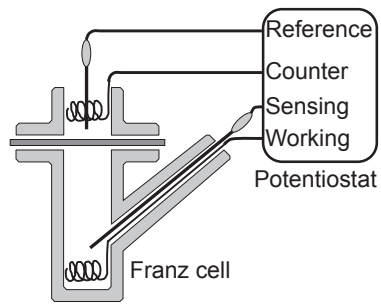

FIGURE 2.4. Four-electrode experimental set-up for impedance measurements.

In paper III, the impedance experiments were performed with the experimental set-up shown in Figure 2.4. A measurement is performed by applying an alternating sinusoidal potential (voltage) between the working and counter electrodes. A consequence of the applied potential difference is that a response current is generated between the counter and working electrodes. This represents the current that flows through the Franz cell between the reference and sensing electrodes, which has to pass the skin membrane (if it is mounted in the cell). In addition, the potentiostat records the potential difference developed between the sensing and reference electrodes.

At a particular frequency, f, the potential difference and the current signals between the sensing and reference electrodes may have a phase difference. The ratio of the potential (here input) and the current (here response) signals is defined as resistance R if the phase shift is zero. If the phase shift is 90° the ratio is equal to $1/(2\pi fC)$ where C is the capacitance. The impedance Z is usually represented as a

vector in the complex plane with real and imaginary axes. The in-phase response (no phase shift) is given by the real part of the impedance, while the out-of-phase represents the imaginary part (Figure 2.5, left). In this case, the resistance corresponds to the real part of the impedance, while the imaginary part is zero, $Z = R - j0$ ($j = \sqrt{-1}$). For the capacitance the real part is zero and the impedance is described by $Z = 0 - j1/(2\pi fC)$. The impedance of an ideal resistor is a vector of length R coinciding with the real axis, while the ideal capacitor is a vector with direction parallel to the imaginary axis (Figure 2.5, left). The impedance of electrical circuits, combining R and C, correspond to vectors, which move with f in the complex coordinates leaving a trace described by complex numbers $Z = Z_{Re} - jZ_{Im}$. For example, the impedance of a parallel configuration of both a resistor and a capacitor results in a semicircle with the center located on the real axis.

The impedance properties of the SC membrane contain both resistive and capacitive elements, which can be modeled with equivalent circuits of varying complexity (92, 111, 113-115). In paper III, the impedance data are characterized by the equivalent circuit shown in Figure 2.5 (middle), consisting of a leading resistor for the electrolyte solution in contact with the skin membrane and a resistor in parallel with a CPE (constant phase element), sometimes referred to pseudo capacitance. As seen in Figure 2.5 (right) the electrolyte resistance is given by the real part of the impedance when the frequency approaches infinity, while the real part of the impedance is dominated by the skin membrane resistance when the frequency approaches zero. The CPE is an empirical circuit element, which reflects non-ideal properties of a real system (116, 117). In paper III we used a graphical representation to determine an effective capacitance of the SC membrane from the CPE. This method is not associated with any fitting parameters as the effective capacitance is calculated from the imaginary part of the high frequency impedance data, where the impedance response most strongly reflects the capacitance in comparison to the resistance. In this region the CPE is expected to approach ideality and thus adequately represent a capacitor (118).

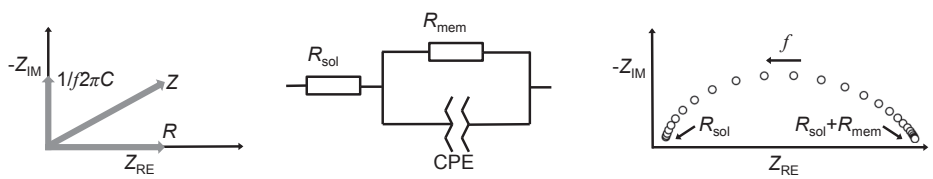

FIGURE 2.5. Vector representation of the impedance Z in the complex plane (left), equivalent circuit used in paper III (middle), and impedance data, in the complex plane, of a skin membrane in contact with PBS buffer (right). Each data point corresponds to a specific frequency f and the arrow indicates the direction of increasing f. At high frequencies Z_{Re} represents R_{sol} and at low frequencies $Z_{Re} = R_{sol} + R_{mem}$.

X-ray diffraction

X-ray diffraction is a compelling technique to investigate structural features of crystalline materials and colloidal systems. The sample is placed in a primary beam of X-rays, which interact with the electron clouds of the molecules in the sample. A detector records the intensity and position of the scattered X-rays, which depends on the molecular geometry and electron density of the sample. The unit cell, i.e. the smallest 3D unit from which the complete lattice can be generated, describes the diffraction pattern. Constructive interference is observed if the X-rays have the same phase after being scattered by the sample electrons, which according to Bragg's law occurs when $n\lambda=2d\sin\theta$. Small-angle X-ray diffraction (SAXD), as the name suggests, measures the intensity at low angles and provides information on structures with large repeat distances (~ 5-15 nm), such as the repeat distance of a lipid lamellar phase (119). Wide-angle X-ray diffraction (WAXD) detects the intensity at wider angles and delivers information on structures with smaller repeat distances (~ 0.3-1 nm), such as the packing of lipid carbon chains in the subunit cell and structural features of assembled protein structures (119).

All X-ray diffraction measurements in this work were performed at Maxlab in Lund (Sweden) at the Swedish-Danish beamline Cassiopeia (I911-4, λ=0.91 Å) (120). The diffraction data in papers III and IV are presented as plots of the scattering intensity as a function of the scattering vector $Q=4\pi\sin\theta/\lambda$. For a lamellar phase, the diffraction peaks are located at equidistant positions in the Q space and the position of the nth order diffraction peak is related to the repeat distance d of the lamellar phase according to $d=2\pi n/Q_n$.

Dynamic vapor sorption microbalance

Results from DVS (Surface Measurements Systems Ltd., London, U.K.) measurements are not included in any of the papers, but presented in the thesis summary. In a DVS experiment, the sample is placed on the microbalance, which continuously logs the sample weight at a selected and controlled RH. The RH is controlled by a stream of humidified nitrogen gas. Here, all measurements were performed at 32 °C with a humidity ramp programmed so that the SC pieces were equilibrated at 80% RH, then at 98% RH, and finally dried at 0% RH. Equilibrium was confirmed by that the sample weight remained unchanged at each RH for several hours. The results are presented as the water content, defined as $(m_{sc} - m_{sc,dry}) / m_{sc}$ where m_{sc} is the total mass of the sample at a certain time point and $m_{sc,dry}$ is the dry weight of the total sample measured at 0% RH.

Dry SC sheets (~ 0.5 mg) were placed in 2 ml of solution, with different solutes, for either 2 h or 24 h at 32 °C. Next, the SC pieces were shaken in air by holding

them with forceps to remove excess solution. In the case of glycerol or urea solutions, the SC sheets were washed gently in PBS solution to remove excess formulation before shaken. Finally, the SC samples were placed in the DVS sample holder.

An experimental consideration related to the preparation of SC samples is the choice of solution to use in this step. We have used PBS buffer to rinse the trypsinated SC tissue. In the literature, pure water is often used for the corresponding preparation. If the SC sample is equilibrated in vapor with defined RH in a later step, the choice of solution in the preparation step will influence the water content of SC, mainly due to presence or absence of buffer ions in the SC sample. This can lead to a notable difference in the SC water content, which is illustrated in the DVS data in Table 2.1. Potentially, this will influence the molecular structure or dynamical properties of the SC components. This issue was not investigated in detail in this thesis work. Still, the SAXD data in paper III, and below, suggest that the water content influences the occurrence of phase separated crystalline cholesterol in SC *in vitro*.

Table 2.1. SC water content (wt%) at 80% and 98% RH. SC samples were soaked in different solutions for 24 h before equilibrated at controlled RH and 32 °C. Salt concentrations are given in mM.

Type of solution	80% RH	98% RH
Milli-Q water	14	24
Phosphate buffer (5.1 Na_2HPO_4, 1.5 KH_2PO_4, pH 7.4)	14	28
131 NaCl in milli-Q water	21	48
PBS (131 NaCl, 5.1 Na_2HPO_4, 1.5 KH_2PO_4, pH 7.4)	23	45

Isothermal sorption calorimetry

In paper V we used an isothermal sorption calorimeter (121, 122) to obtain sorption isotherms of pure glycerol, urea, PCA, and UCA. This method involves a twin calorimeter, each equipped with a double chamber calorimetric cell. In the measuring calorimeter, one chamber contains pure water while the other contains the sample. The two chambers are connected by a tube to allow for water vapor diffusion from the vaporization chamber to the sample chamber. From the thermal power of vaporization, measured in the vaporization chamber, one can obtain the sorption isotherm in the form of water content as a function of RH. The thermal power, measured in the sample cell, is related to the water sorption of the sample, which can be quantified by the partial molar enthalpy of sorption (mixing of water) as a function of water content. This method therefore provides a more complete thermodynamic characterization of the sorption process, as compared to e.g. DVS.

3 Interplay between hydration and skin permeability

This chapter gives a brief introduction of the scientific questions posed in papers I-III and summarizes key results and their practical significance. The chapter ends with a discussion aiming to connect these observations to obtain a more complete picture of the effect of hydration on skin permeability. Additional unpublished SWAXD results are also included in this chapter.

A water gradient can be used to regulate drug transport across skin

Water diffusion across SC is strongly dependent on the external RH, which effectively determines its degree of hydration (79, 80). In particular, water flux across SC is not proportional to the gradient in water activity, which would be expected if the properties of the SC membrane remained unaffected by hydration (79, 80). The non-linear relation between the water flux and the water activity gradient implies that hydration can induce alterations of the SC structure and/or changes of the phase properties of the SC components, which ultimately determines the diffusional resistance (123). This implication was the working hypothesis for paper I, where a systematic investigation of the interplay between the water gradient across the skin membrane and its permeability was performed. In these experiments, the water activity in the receptor solution was constant at physiological conditions, while the water activity in the donor formulation ($a_{w,d}$) was regulated. To explore if changes of $a_{w,d}$ influence the permeability likewise for molecules with different lipophilic characteristics we employed two model drugs; Mz (log P=0.0) and MeSA (log P=2.5) (49, 50). We also investigated how the skin permeability is affected by sequential variations of $a_{w,d}$ by switching between a low and a high value of $a_{w,d}$.

As demonstrated in Figure 3.1, the $a_{w,d}$ has a clear effect on the permeability of both Mz and MeSA. Figure 3.2 shows that the repeated alterations of $a_{w,d}$ between a low and high value leads to largely reversible changes in skin permeability for both model drugs. The effect is more pronounced for Mz with a 6-7 fold increase in flux as most, while the corresponding increase for MeSA is 2-3 fold.

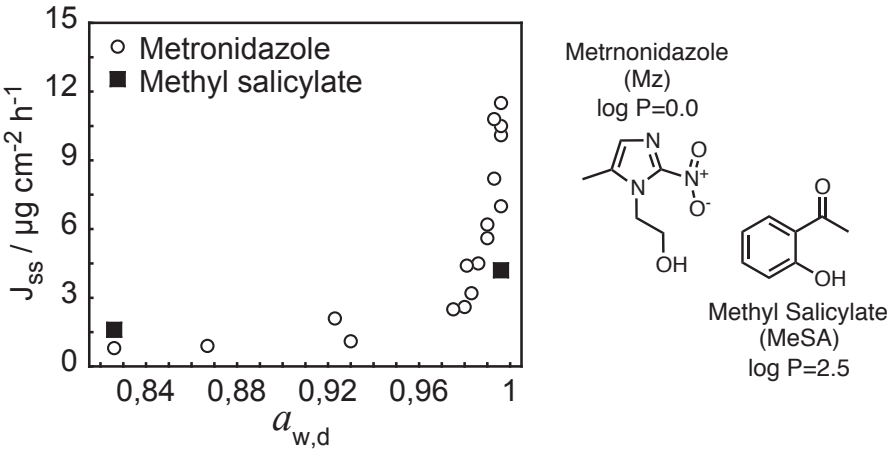

FIGURE 3.1. Steady state flux of Mz and MeSA increases as the water activity in the donor formulation ($a_{w,d}$) increases (left). Chemical structures of Mz and MeSA (right). Data of log P from (49, 50).

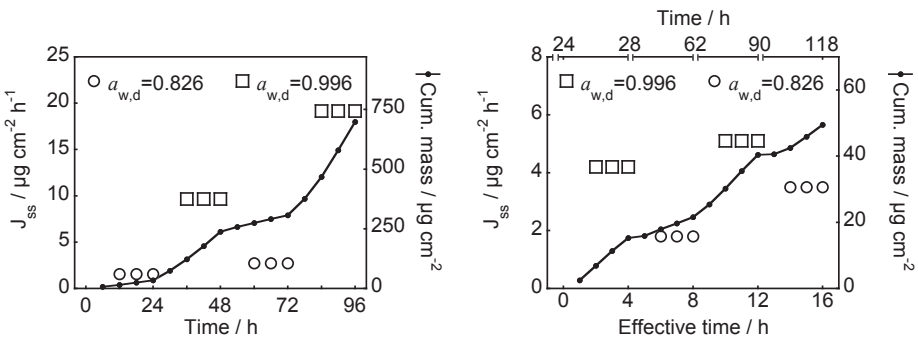

FIGURE 3.2. The water activity in the donor formulation ($a_{w,d}$) has a clear effect on the skin permeability of Mz (left) and MeSA (right). Open symbols show steady state flux (left y-axis) and closed symbols connected with line show the cumulative permeated mass (right y-axis).

Additional experiments were performed, where the water activity was regulated to 0.826 (65wt% PEG in PBS) in both the donor *and* the receptor solutions. This resulted in a dramatic reduction of the skin permeability of Mz with a steady state flux of only 0.18±0.03 µg cm^{-2} h^{-1} (n=6, unpublished data). This flux is around 50 times lower as compared to the flux when PBS solution is present on both sides of the membrane. Repeating the same experiment with silicone membranes instead of skin membranes gave a steady state flux of 2.2±0.2 µg cm^{-2} h^{-1} (n=3, unpublished data). This flux of Mz, over inert silicone membranes, is identical to the corresponding flux of Mz when PBS solution is used as receptor phase (see paper I) and strongly suggests that the reduced skin permeability is related to the effect of dehydration.

Practical significance

The results in paper I demonstrate the interplay between the external water activity (here $a_{w,d}$) and the drug permeability of skin and highlight the importance of defining and controlling the water activity in (trans)dermal formulations. Several studies, both *in vivo* and *in vitro*, have shown that increasing the hydration by occluding the skin surface with an impermeable dressing leads to increased skin permeability for most molecules with a molecular weight below 500 Da (77, 78, 124). Still, the detailed relation between the gradient in water activity and the change in skin permeability cannot be elucidated from studies with only two experimental conditions, i.e. occluded and non-occluded skin. Using a simple experimental set-up with well-defined boundary conditions allowed for a systematic characterization of this interplay. The results in Figure 3.1 for Mz provide a detailed picture of the boundary conditions required making use of the skin occlusion effect, or alternatively, the conditions needed to minimize the skin permeability of e.g. toxic substances. The results in Figure 3.2 demonstrate how hydration can be used to regulate the skin permeability of drugs with different lipophilic characteristics in a reversible manner. This is a relevant result for transdermal applications, which potentially could be used for hydration regulated temporal drug delivery.

Skin impedance under the influence of a varying water gradient

In paper III we explored how the skin membrane electrical properties are influenced by variations of the external water activity ($a_{w,d}$). The aim was to relate skin membrane resistance (R_{mem}) and effective capacitance (C_{eff}) to skin permeability under identical hydration conditions. In this work we followed the experimental procedure of the switch experiments in paper I (cf. Figure 3.2), but instead of measuring drug flux we continuously recorded impedance data of the skin membrane. The results in Figure 3.3 demonstrate how the membrane resistance and effective capacitance are reversibly regulated by sequentially changing the water gradient. The values from the plateau regions of the final hours of each time period show relatively stable values of R_{mem} and C_{eff}. When comparing the average values from the plateau regions, the skin membrane resistance is 14 times higher for the less hydrated skin membrane, while the effective capacitance in average is 1.5 times higher for the hydrated skin membrane (paper III).

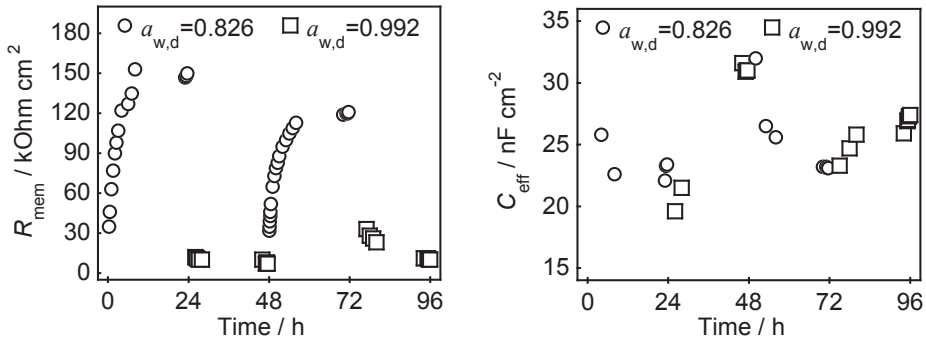

FIGURE 3.3. The water activity gradient has a strong influence on the membrane resistance (left) and effective capacitance (right).

Practical significance

Previous investigations have demonstrated an inverse correlation between passive diffusion of hydrophilic molecules and membrane resistance (93, 125-127). Going one step further, our results show that there is a correlation between the changes of the skin membrane resistance and the steady state flux of Mz and MeSA under the influence of a varying water gradient. In addition, the effective capacitance is shown to correlate with the flux data. Combined, our results show that impedance measurements provide important and complementary information on how skin permeability is affected by external parameters, such as the water gradient.

Hydration influences the dynamics of SC molecular components

A detailed description of how variations of the external water activity ($a_{w,d}$) influence the SC permeability and impedance properties requires a molecular characterization of how the SC components are affected by hydration. In paper II we employed natural-abundance ^{13}C PT ssNMR to approach this problem. Establishing an assignment of the multitude of resonances in the complex ^{13}C spectrum of SC was a prerequisite for data interpretation. This was realized from combined experiments on intact SC and isolated corneocytes. The isolated corneocytes, which contain a minor fraction of covalently bound lipids of the CE, was obtained after lipid extraction of SC. Measurements on the extracted SC lipids were also performed, but due to potential contamination or degradation (Figure S1, paper II) we instead utilized a mixture of SC model lipids, consisting of ceramides, fatty acids, and cholesterol (cf. Figure 1.3). Systematic comparison of these spectra, with consideration to the chemical composition of different proteins and lipids in SC, and resorting to previous peak assignments on relevant protein

and lipid systems (128-132), allowed for a detailed peak assignment. The assignment of prominent peaks was further confirmed by performing INEPT experiments with varying delay times, from which it is possible to differentiate between CH_3, CH_2, and CH resonances. The assignment is detailed in paper II.

Next, we investigated the effect of hydration on the SC molecular dynamics by focusing on signature peaks of lipid and protein components, which are labeled in Figure 3.4 (data from paper II and III). The dynamics of the terminal domains of the keratin filaments can be probed by the glycine and serine residues. Excluding the carbonyl carbons, glycine has one carbon (Gly C_α), while serine has two (Ser C_α, and Ser C_β). The INEPT peaks from these residues are present at 85% RH and above, but totally absent at lower RH. This shows that these molecular segments are mobile at 85% RH and above (cf. Figure 2.3, fast regime and case iii), but rigid at 80% RH and below (cf. Figure 2.3, slow regime or fast regime and case i). The mobility of the backbone of the coiled-core of the keratin filaments can be probed by the leucine and lysine residues, which have four carbons each (not including the carbonyl). However, it is only the Leu C_β and Lys C_ε segments that resonate above the crowded aliphatic region and thus less influenced by other peaks. The prominent CP peak from Leu C_β and Lys C_ε is present at all RHs, showing that the protein backbone remains in a rigid state irrespective of hydration (cf. Figure 2.3, slow regime). The most prominent lipid peak is from the all-trans configurated $(CH_2)_n$ segments of rigid hydrocarbon chains (133). The intensity ratio of CP over DP signal (I_{CP}/I_{DP}) from the all-trans peak decreases upon hydration, still it is clear that even in the most hydrated state the majority of lipids remains in a rigid state (cf. Figure 2.3, slow regime or fast regime and case i). The $(CH_2)_n$ segments of hydrocarbon chains with a distribution of trans/gauche confomers (133), and the terminal carbons of the hydrocarbon chains, ωCH_3 and

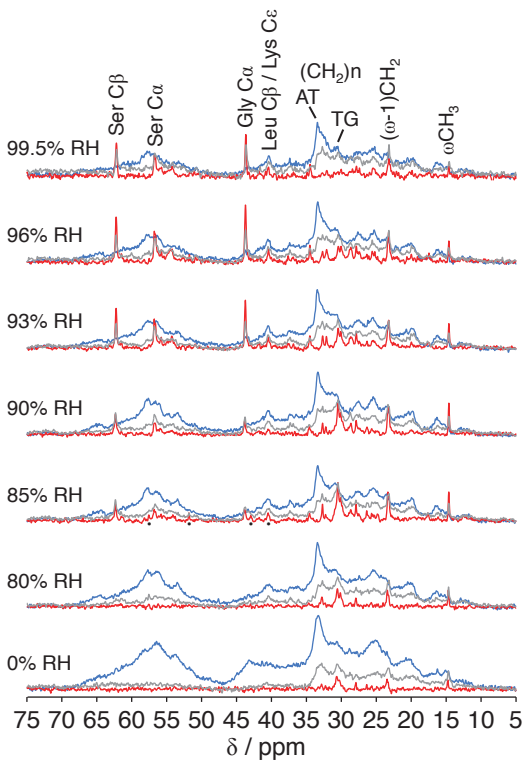

FIGURE 3.4. PT ssNMR spectra (DP in grey, CP in blue, and INEPT in red) of SC at varying RH. AT is all-trans and TG is trans/gauche.

(ω-1)CH_2, are relevant resonances for probing lipid mobility.

At 0% RH all these lipid segments show INEPT signal from a minor fraction of mobile lipids (cf. Figure 2.3, fast regime and case iii). The intensity ratios of INEPT over DP signal (I_{INEPT}/I_{DP}) from the terminal ωCH_3 and (ω-1)CH_2 resonances increase steadily up to 85% RH, remain virtually unchanged up to 96% RH, and decrease at 99.5% RH. This trend is not seen for the I_{INEPT}/I_{DP} ratio of the $(CH_2)_n$ peak, which is highest at 85% RH, marginally decreased at 90% RH, then continuously reduced at higher RH.

The results in Figure 3.4 from the lipid signature resonances at varying RH are intriguing. How can it be that the INEPT signal from these resonances at 0% RH is similar, or even higher, as compared to the spectra at 96% or 99.5% RH, at the same time as the I_{CP}/I_{DP} ratio decreases for the all-trans $(CH_2)_n$ peak? Our explanation is that hydration between 0% and 85% RH leads to fluidization of foremost lipid species with shorter hydrocarbon chains, which increases the INEPT signal from all lipid signature peaks. At higher RHs, the fraction of mobile lipids increases by incorporation of lipids with longer hydrocarbon chains, together with cholesterol, which act to decrease the overall mobility of the fluid lipid fraction due to the inherently slower dynamics of these bulkier species (e.g. going from the fast dynamic regime towards the fast-intermediate regime in Figure 2.3). Thus, mobilization of long-chain lipids leads to a reduction of the INEPT efficiency, especially from segments contributing to the $(CH_2)_n$ resonance. Here, it can be noted that the INEPT peaks marked with dots in Figure 3.4, which are only present at 85% RH, can be assigned to mobile cholesterol. This is a further indication of that hydration can affect the composition of the fluid lipid fraction. Figure 3.5 serves as a summary of the hydration effect on the SC molecular dynamics. The color-coded fields are scaled from white (zero I_{INEPT}/I_{DP} ratio) to red (max. I_{INEPT}/I_{DP} ratio).

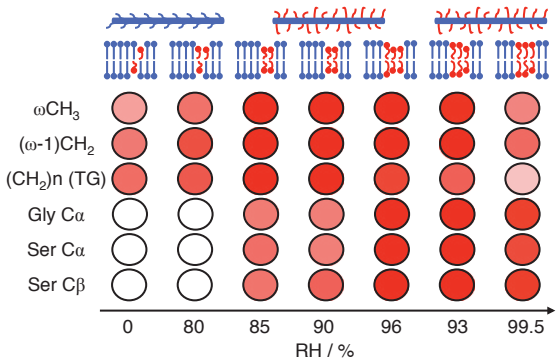

FIGURE 3.5. Color-coded I_{INEPT}/I_{DP} ratios for lipid and protein signature peaks at varying RH, from 0% to 99.5%. White is defined as zero I_{INEPT}/I_{DP}, while red is defined as the maximum experimental I_{INEPT}/I_{DP} ratio for a particular signature peak. The schematics illustrate how the intensity changes can be explained in terms of changed lipid and protein mobility.

Practical significance

A great benefit of PT ssNMR is that it detects mobile components even when those are occurring in minor fractions, while it simultaneously gives information on the rigid components in the very same sample. This work illustrates this benefit, and how it is possible to exploit the peak assignment and map dynamical changes of different SC molecular components under varying hydration conditions. In paper II we further illustrate how the SC molecular dynamics can be probed by PT ssNMR at varying temperatures. The molecular information obtained in this work improves the understanding of, for example, why the SC become non-elastic and brittle in the dry state (63), and why hydration and temperature increases the skin permeability (79, 80, 134, 135). Potentially, this technique can be used to increase the knowledge of common skin disorders, like psoriasis and atopic dermatitis, which are associated with altered SC biophysical properties (136, 137), or alternatively to explore the effects of various transdermal drug applications (e.g. penetration enhancers, etc.) on the SC.

The effect of hydration on the SC structure

A complement to the results in paper II is provided from SWAXD measurements on SC. X-ray diffraction experiments were performed at 0%, 80%, 90%, 96%, and 99.5% RH (paper III and unpublished data), following the sample preparation protocol given in paper III. The results are compiled in Table 3.1. In general the SAXD data show broad peaks or shoulders on the descending diffraction curve, which makes it uncertain to specify the exact diffraction position. In Table 3.1 the values gives the location of the center of the peaks/shoulders or, in the case of the first order diffraction, the interval of the shoulder location. Taken together, the SAXD data suggest that the lipid lamellar structures have a spacing of ~ 13 nm, while the WAXD data consistently show a peak at 0.41 nm, attributed to hexagonal packing of the hydrocarbon chains. This is consistent with previous diffraction studies on pig SC (32).

Table 3.1. SAXD and WAXD (nm) data of SC at 32 °C and varying RH. Data at 0%, 90%, and 96% RH are unpublished, while 80% and 99.5% RH are from the supporting material of paper III. WAXD was not performed at 0% RH.

RH	~12.6 nm lamellar phase (12.6, 6.3, 4.2, 3.2)	Crystalline cholesterol	Chain packing	Protein interchain distance
0%	-	3.4	n.a.	n.a.
80%	6.3, 4.2	3.4	0.41 (hex.)	0.95
90%	6.3, 4.4	-	0.41 (hex.)	1.00
96%	12.0-12.6, 6.3, 4.3 (5.0?)	3.4-3.5	0.41 (hex.)	1.02
99.5%	9.8-12.6, 6.3, 4.4, 3.2	-	0.41 (hex.)	1.02

We note that a short lamellar phase with ~ 6 nm spacing, in coexistence with the ~ 13 nm lamellar phase, has been suggested to be present in SC (29, 32). However, from our data this cannot be confirmed as no higher order diffractions from a ~ 6 nm phase are observed. The diffraction curve at 96% RH shows an unidentified peak at 5.0 nm spacing. The spacing between the keratin protein chains (81, 138) increases from 0.96 nm to 1.0 nm when the RH increases from 80% to 90%, which coincide with the abrupt mobility increase of the keratin terminals in the same RH interval (cf. Figure 3.4). A diffraction peak ascribed to phase separated crystalline cholesterol (32), corresponding to the spacing from a bilayer of cholesterol monohydrate (139), is present at 0%, 80%, and 96% RH. The intensity of this diffraction peak at 96% RH is weak, while no signs of crystalline cholesterol is observed at 90% and 99.5% RH. This indicates that hydration influences the appearance of phase separated cholesterol, potentially by dissolving a fraction of cholesterol into the fluid lamellar lipid structures at higher RH. The occurrence of crystalline cholesterol in diffraction data of SC seems to be related to sample variability, sample preparation, and sample history. As shown in Figure 4.1 (below), this peak is present for all samples pretreated in various solutions (i.e. not equilibrated in humidified vapor). Also, in all cases the diffraction from crystalline cholesterol disappears after heating the SC to 90 °C and allowing the samples to cool down at 32 °C, see paper IV and other studies (32). Some further remarks related to the presence of crystalline cholesterol in SC are found in paper III.

Molecular insight into the changes of SC permeability upon (de)hydration

The steady state flux results of Mz and MeSA clearly demonstrate that skin (de)hydration, regulated by the external water activity ($a_{w,d}$), has a strong influence on the SC permeability (paper I). In addition, the $a_{w,d}$ can be used to sequentially increase or decrease the permeability (paper I), and this effect can be correlated to the qualitative changes of the skin membrane resistance and effective capacitance (paper III). Finally, increased SC hydration (i.e. elevated SC water content) leads to mobilization of the non-aqueous SC components (paper II). The emerging picture, summarized in Figure 3.5, show how hydration influences the dynamics of the SC components, which combined with the diffraction data in Table 3.1, provide a molecular understanding of the macroscopic flux and impedance results.

The SC permeability and electrical resistance is primarily attributed to the solubility and diffusional mobility of model dugs and ions in the different regions of the composite SC membrane. Both these factors depend on the phase properties of the SC components and their organization within the SC (9, 123). The phase properties of molecular matter are strongly related to its molecular dynamics (rotational diffusion rate and order parameter) as characterized by PT ssNMR (84, 106, 107).

From the combination of data, presented in papers I-III, we suggest that the increased permeability of the model drugs and the decreased skin membrane electrical resistance are related to hydration induced mobilization of the SC lipid and protein components, leading to increased solubility and lowered diffusional resistance. The detailed data of Mz transport as a function of water activity (Figure 3.1) show that the abrupt increase in flux occurs above $a_{w,d} \sim 0.96$. This is considerably higher than the corresponding RH region where the keratin filament terminals become mobile (Figure 3.4), and show the largest increase in protein chain spacing (Table 3.1). Indeed, the most prominent change in SC molecular dynamics above $a_{w,d} \sim 0.96$ (96% RH) is the reduced I_{INEPT}/I_{DP} from the lipid segments (Figure 3.4 and 3.5), which we ascribe to reduced dynamics from mobilization and incorporation of long-chain lipids into the fluid fraction. In other words, the fluid fraction increase in size in this hydration region, simultaneously as the average dynamics in this lipid fraction decreases. These observations point to that the fluidization of lipid species is important to consider in relation to the increased flux and the decreased skin membrane resistance. It is likely that the fluid fraction of lipids represents a route with lower diffusional resistance within the main fraction of solid lipids and that this pathway becomes more influential at high SC hydration.

The effective capacitance can be related to low conductive regions in SC that impede ion transport. In the literature, the SC capacitance has been attributed mainly to the extracellular lipid lamellae and the lipid-protein interface of the CE (93, 111, 112, 140). The SC capacitance has also been related to a double layer of dissociated species of the SC (lipids or proteins), which are charge-balanced by electrolyte ions (114). From our data in paper III we cannot distinguish between these two mechanisms, as both are consistent with the data

Note that SC samples prepared in solution with a_w, adjusted with PEG in PBS solution, have virtually the same dynamical and structural properties as compared to SC prepared at the corresponding RH (paper III). Therefore it is valid to relate the flux and impedance results at a specific a_w to the NMR data at corresponding RH.

A difference in the relative increase in flux between Mz (log P=0.0) and MeSA (log P=2.5) was observed upon hydration (Figure 3.1 and 3.2). A reasonable explanation of this is that polar domains of SC swell upon hydration, which would influence polar and apolar molecules differently. It is known that the corneocytes can swell substantially upon hydration, mainly in the vertical dimension (28, 141-144). Studies employing various imaging/microscopy techniques have shown that SC hydration with pure water or buffer solution can lead to creation of aqueous inclusions, which have been suggested to form in pockets of degraded corneodesmosomes (104, 142, 144-146). These isolated structures (corneocytes and aqueous inclusions) could thus represent local regions of high flux resistance for hydrophobic substances due to unfavorable solubility. This would act to increase the diffusional path length (tortuosity) of apolar molecules, like MeSA. However, these structures would not have a significant effect on the diffusional resistance of neither more polar drugs, like Mz, nor ions due to their high solubility in these polar regions. The main message is that both model drugs in all situations have to be transported across the continuous lipid regions in an intact SC membrane, irrespective of the presence of isolated polar structures.

4 Influence of osmolytes on SC in reduced hydration conditions

This chapter gives a short introduction of the scientific questions investigated in papers IV and V, with a summary of key results and their practical significance. A more general discussion of the effects of natural moisturizers on the SC molecular dynamics follows. The chapter ends with a discussion focusing on the osmolytes glycerol and urea and how they influence SC permeability, molecular dynamics, and molecular structure. Unpublished DVS results are also included in here.

Glycerol and urea increase skin permeability in reduced hydration conditions

Glycerol and urea are components of the NMF and also used in commercial skin care products, for example in treatment of dry skin. The beneficial function of these compounds has been related to their capability to increase SC hydration (147-149). With respect to this we ask the question: Is it only the amount of water that determines the SC functionality in dry skin? We believe it is more relevant to consider the physical state of the SC components. This can be affected by the water content in SC, as shown in papers I-III and in other studies (79-82). Interestingly, it has been demonstrated that glycerol and urea can maintain fluidity of model lipid systems in dry conditions, where solid structures otherwise would form in the absence of these small polar compounds (83, 84, 150). Considering this, we hypothesized that a similar mechanism is important in situations where osmolytes and NMF components are present in SC under dehydrating conditions. In other words, because water and osmolytes may affect the physical state of the SC molecular components in a similar manner it is important to consider the combined effect of both water and osmolyte.

First we ask the question: Do glycerol and urea increase the SC water uptake? We performed DVS measurements to investigate this. It is obvious that *in vivo* studies found in the literature (147-149) differ, as compared to the present DVS experiments, which illustrate another important point. In the *in vivo* case, the formulation, which often contains more ingredients than the osmolyte, is applied over several days, or weeks, and the skin hydration is evaluated with some method.

Examples of different methods are electrical measurements of the skin conductivity (skicon) and capacitance (corneometer), or letting the patient score the feeling of dryness (147-149). Thus, in *in vivo* studies, performed over an extended time, response mechanisms may involve, for example, both physical and biochemical alterations of the SC membrane. In the present DVS experiments, the SC was separated from the viable epidermis to allow for focus on the SC water uptake. The water content is measured at a defined RH after pretreatment of the SC in a formulation that contains either glycerol or urea.

Table 4.1. SC water content (wt%) at 80% and 98% RH. SC samples were soaked in neat PBS solution and PBS solution with either 20wt% glycerol or urea for 2 h or 24 h before equilibrated at controlled RH and 32 °C.

Type of solution	80% RH	98% RH
PBS (131 mM NaCl), 24 h	23	45
20wt% Glycerol 2 h	25	49
20wt% Glycerol 24 h	26	50
20wt% Urea 2 h	25	54
20wt% Urea 24 h	31	62

It is shown that the presence of glycerol or urea leads to an increased water content in SC, but the effect is perhaps not as substantial as one would expect considering the hygroscopic properties of these substances (Table 4.1). For example, at 80% RH the water content of the SC sample prepared in PBS is 23wt%, while the corresponding water amount of the glycerol or urea treated samples (24 h) are 26wt% and 31wt%, respectively. This increase in SC water content is moderate if it is assumed that glycerol or urea penetrates the SC and is present at a few wt% in addition to water. In this case, the influence of the total fraction of polar molecules (osmolyte plus water) on the SC phase properties may be more relevant to consider.

If osmolytes act to retain fluidity of the SC components this would likely influence the permeability. The aim of paper IV was to investigate this hypothesis on a macroscopic level by determining how glycerol and urea influence the SC permeability of Mz at varying hydration conditions. This was done by a similar methodology as in paper I, but instead of regulating $a_{w,d}$ with only polymers in neat PBS we used glycerol and urea, or a combination of one of these osmolytes and PEG.

By adding these small molecules to the model drug formulation, the a_w in the formulation decreases as shown in Figure 2.1. When the formulation is placed on top of the skin membrane, the lowered $a_{w,d}$ will thus act to dehydrate the SC at the same time as glycerol and urea can penetrate the SC and influence the barrier properties. Figure 4.1 (left) shows how the steady state flux of Mz across skin membranes in contact with formulations with varying amount of glycerol or urea is influenced by the $a_{w,d}$. We conclude that glycerol and urea maintain high SC

permeability at reduced $a_{w,d}$, which is in clear contrast to the situation when $a_{w,d}$ is regulated with only PEG in neat PBS (results from paper I included for comparison). In Figure 4.1 (right), it is demonstrated that addition of PEG to formulations containing 20wt% glycerol or urea leads to a gradual decrease of Mz flux, similar to when only PEG is added to neat PBS. However, by comparing data points at similar $a_{w,d}$, it is clear that the formulations, containing glycerol or urea, are associated with higher flux of the model drug. In fact, the presence of glycerol or urea in the formulations leads to a clear change in the flux profile at varying $a_{w,d}$, where the abrupt decrease in drug flux is shifted towards lower $a_{w,d}$ (i.e. higher flux at more dehydrating conditions).

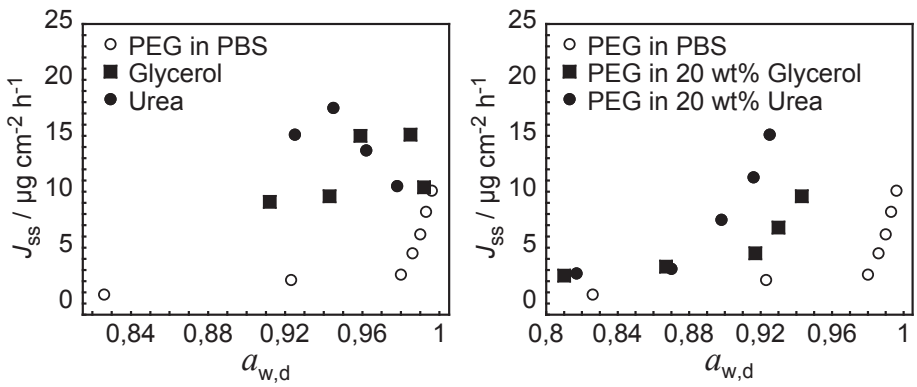

FIGURE 4.1. Steady state flux of Mz remains high when the $a_{w,d}$ is regulated by glycerol or urea (left), while the presence of these osmolytes leads to higher Mz flux when the $a_{w,d}$ is adjusted by PEG when comparing similar hydration conditions. Data of PEG in PBS are from paper I.

Practical significance

The results in paper IV show how glycerol and urea can be used to control the skin permeability in relation to the external water activity ($a_{w,d}$). Extrapolated to a real situation, the results demonstrate how glycerol and urea may be used to substitute for water in transdermal or topical formulations to retain the properties of a hydrated skin membrane in dry conditions. Water has a relatively high vapor pressure compared to glycerol or urea. Therefore, these small polar molecules will be virtually unaffected by evaporation and stay on the skin application site in situations where water evaporates.

The effect of natural moisturizers on SC molecular organization and dynamics

To follow up on the hypothesis that small polar molecules can influence the phase properties of SC molecular components under dehydrating conditions, we performed PT ssNMR and SWAXD measurements on SC in the presence of NMF.

How glycerol, urea, UCA, and PCA influence the dynamics of SC molecular components

In the PT ssNMR experiments (paper V), pulverized SC samples were prepared with a known amount of glycerol, urea, PCA, or UCA (wt% based on dry SC weight) and equilibrated at 80% RH and 32 °C. Figure 4.2 shows PT ssNMR spectra of SC with 20wt% of these substances. For comparison, spectra of "pure" SC at 80% RH and 96% RH are included in Figure 4.2.

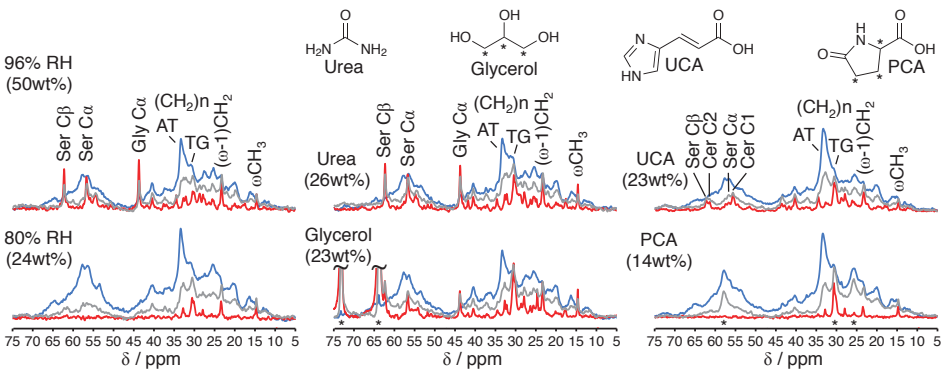

FIGURE 4.2. PT ssNMR spectra (DP in grey, CP in blue, and INEPT in red) of pure SC at 80% RH and 96% RH, and with 20wt% urea, glycerol, UCA, and PCA at 80% RH. SC water content is given in parenthesis. AT is all-trans and TG is trans/gauche. Glycerol and PCA ^{13}C resonances are marked with asterisks.

A first observation is that all NMF molecules, except PCA, influence the dynamical properties of the SC molecular components at 80% RH. The presence of glycerol or urea leads to a clear increase of the I_{INEPT} signals from protein and lipid components, as compared to the SC sample without these substances at 80% RH. Indeed, the spectra of SC with glycerol or urea are very similar to the spectra of pure SC at 96% RH. The prominent INEPT signals from the Gly C_α, Ser C_α, and Ser C_β segments in the samples with glycerol or urea show that the keratin filament terminals are mobilized (cf. Figure 2.3, fast regime and case iii). Still, the clear CP signal from rigid Leu C_β and/or Lys C_ε segments around 40 ppm (cf. Figure 3.4) suggests that the coiled-core of the keratin filaments is solid in both these samples (cf. Figure 2.3, slow regime).

The INEPT signals from the lipid signature resonances, i.e. $(CH_2)_n$, ωCH_3, and $(\omega\text{-}1)CH_2$, are enhanced in the samples with either urea or glycerol, as compared to the SC sample without NMF at 80% RH, implying increased lipid mobility (cf. Figure 2.3, fast regime and case iii). Taken together, the results clearly demonstrate that both glycerol and urea act to retain the molecular mobility of the SC components at reduced hydration conditions, where the molecular components are more rigid in the absence of these molecules.

The spectra of SC with UCA show INEPT signal enhancement at resonances around 35, 56, and 61 ppm, which can be assigned to the ceramide (CER C1, C2, αCH_2) and fatty acid (αCH_2) headgroup carbons (see paper V). This implies that presence of the less polar UCA molecule influences the mobility of the extracellular SC lipids under the present experimental conditions. The INEPT signal around 41 ppm can be assigned to cholesterol (C12/C24) and is a further indication of that UCA affects the apolar lipid regions of SC. In comparison to the pure SC sample at 80% RH, also the INEPT signal at the Gly C_α, Ser C_α, and Ser C_β resonances are more enhanced. Still, these peaks are less increased as compared to the spectra from the SC samples with glycerol or urea.

In paper V, we performed additional measurements at lower NMF concentrations. Figure 4.3 presents a compilation of the I_{INEPT}/I_{DP} ratios for the signature resonances from these experiments along with schematic interpretation of the data. The main conclusion is that the presence of urea or glycerol leads to similar molecular dynamics as observed for the close to fully hydrated SC sample in absence of these molecules. In addition, the effect of UCA differs in that it affect the dynamics of carbon segments in ceramides, fatty acids, and cholesterol. Finally, PCA does not have any effect on the SC molecular mobility under the experimental conditions.

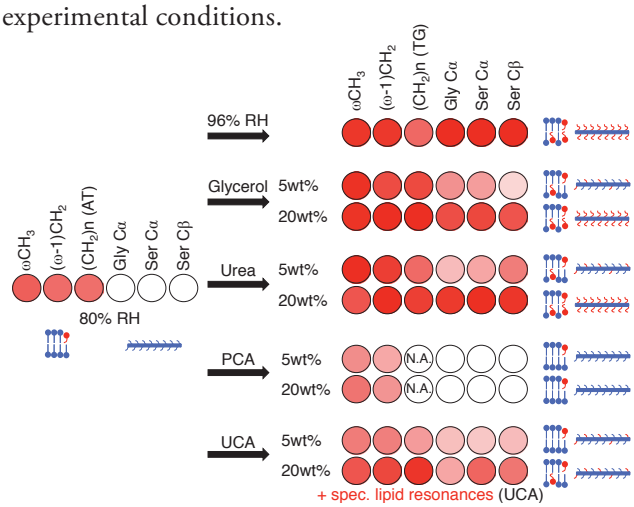

FIGURE 4.3. Color-coded I_{INEPT}/I_{DP} ratios for lipid and protein signature peaks of SC samples at 80% RH with urea, glycerol, PCA, and UCA. Pure SC at 96% RH is included for comparison. White is defined as zero I_{INEPT}/I_{DP}, while red is defined as the maximum experimental I_{INEPT}/I_{DP} ratio for a particular signature peak. The schematics illustrate how the intensity changes can be explained in terms of changed lipid and protein mobility.

Similar SC structure at dehydrating conditions in the presence of glycerol and urea

In the SWAXD measurements (paper IV), the SC sheets were pretreated for 24 h in neat PBS (a_w=0.992), 20wt% glycerol in PBS (a_w=0.943) or 20wt% urea in PBS (a_w=0.925) for 24 h at 32 °C. The diffraction data for all these samples are similar (Figure 4.4). However, the curves from the SC sample pretreated in urea formulations show generally weaker diffraction. Particularly for the broad peak ascribed to the protein interchain spacing around 1 nm (WAXD) (81, 138), which indicates a reduced fraction of solid proteins structures in the urea sample. Possibly, this can explain the observed relative increase in water uptake for the SC samples pretreated in 20wt% urea for 2 h or 24 h (Table 4.1), implying that urea affects the SC structure over time, leading to a higher capacity of the SC components to take up more water.

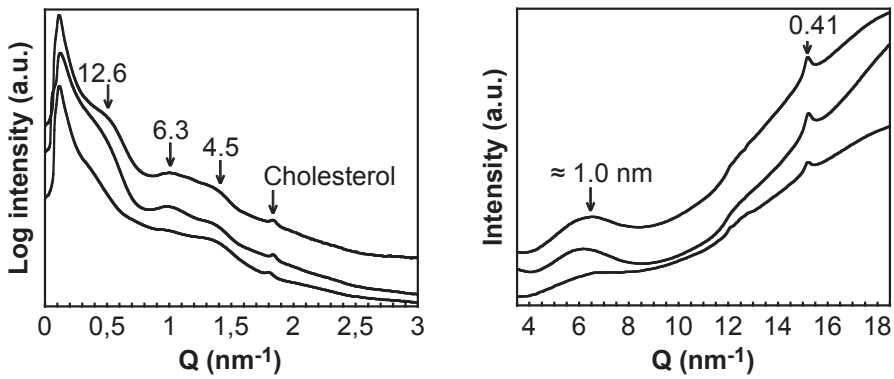

FIGURE 4.4. SAXD (left) and WAXD (right) data from SC samples pretreated in neat PBS solution (middle curves), 20wt% glycerol (top curves), and 20wt% urea (bottom curves) for 24 h at 32 °C. Arrows are located around the center of the broad shoulders/peaks and the numbers indicate the spacing of the diffractions.

We interpret the data as the SC lipid organization resembles a lamellar phase of ~ 12.6 nm spacing with hexagonal packing of the acyl chains. This is in agreement with previous diffraction studies on pig SC without the presence of glycerol and urea (32). The spacing of the peak attributed to the interchain spacing of the keratin is at ~ 0.95 nm for the SC samples with glycerol (and urea), and ~ 1.02 nm in the SC sample pretreated in PBS. As shown in Table 3.1, and in other studies (81, 138), this spacing is influenced by the external RH. Considering that a_w is lower in the glycerol and urea formulations, as compared to neat PBS, this shift in spacing may be explained in terms of reduced a_w and thus less space between the protein chains. However, we note that this spacing, when glycerol or urea is present in the SC sample, is similar to the spacing at 80% RH, which implies that it is not only the a_w or RH that may influence the interchain spacing of these protein structures.

Practical significance

Water is a well-known plasticizer of SC, which act to keep the skin pliable (63, 151). Similarly, the NMF substances, and skin care products containing these, can serve to increase skin smoothness and elasticity, and this is often explained by increased SC hydration. The DVS results in Table 4.1 show that pretreatment of SC in glycerol or urea formulations can influence the water content to some degree. In the DVS experiments, water uptake is studied for samples that had been pretreated in a formulation with known composition, and where the content of urea or glycerol in SC is not controlled. This differs from the sample preparation protocol used in paper V, where SC powder was mixed with a known amount of NMF and equilibrated at 80% RH. An important observation in paper V is that the water content is similar for all SC samples at 80% RH, except for the sample with PCA that contains a lower amount of water.

More importantly, in paper V we show that addition of glycerol or urea alters the properties of the SC lipid and protein components. This can indeed be related to SC hydration because the addition of water influences the molecular mobility of SC protein and lipid components as shown in paper II and III. However, the similar SC water content strongly suggests that the influence of urea, glycerol, and UCA on the SC molecular dynamics is not simply explained only by their capability to increase the SC water content. An alternative explanation is that these substances affect the SC molecular mobility by their presence, acting to retain fluidity of the molecular components at dehydrating conditions. Thus, it is most relevant to consider the total amount of polar molecules (water and NMF) in relation to the influence of these substances on the SC properties. The NMF compounds have low vapor pressure and therefore remain in the SC at reduced RH where water evaporates. In this way, the NMF can substitute for the water in reduced hydration conditions in such a way that the SC properties remain largely unchanged as compared to a more hydrated SC state. This is likely an important role of NMF in SC.

Glycerol and urea are classified as humectants with the role to moisturize the skin. We find this terminology to be somewhat misleading in that urea and glycerol have the effect of increasing the mobility of the lipid and protein components at dry conditions, while the water content is almost unchanged. This implication can be related to increasing pliability and softness of SC treated with moisturizers under dry conditions and to the beneficial properties of moisturizers in skin treatment.

Molecular insight into the influence of glycerol and urea on the SC permeability

The experimental conditions of the SWAXD and PT ssNMR experiments are not the same, and also differ from the non-equilibrium situation in the flux experiments. However, the combination of results from these different studies points to that glycerol and urea can retain the physical properties of the SC components at reduced hydration conditions. In the flux experiments this leads to unchanged permeability of the model drug in SC at decreasing levels of $a_{w,d}$ (Figure 4.1, left). This can be related to that the SC structure, as observed from SWAXD, is similar for the fully hydrated SC sample and the SC samples at lower a_w when glycerol or urea is present (Figure 4.4). The results from PT ssNMR complete the picture and show that the SC lipid and protein components are significantly more mobile when glycerol and urea are present, in comparison to the SC sample without these molecules at 80% RH (Figure 4.2). Indeed, the spectra in Figure 4.2, from SC with glycerol and urea, are very similar to the spectra of pure SC at 96% RH, indicating that these substances act to retain the physical properties associated with a more hydrated SC membrane. As discussed in the last section in chapter 3, the presence of fluid molecular components in the SC can act to increase the SC permeability by increasing the solubility of the diffusing molecule and its diffusion coefficient, and thus lower the SC diffusional resistance. Therefore, by retaining fluidity of the SC components at reduced hydration conditions, glycerol and urea act to increase the SC permeability at dehydrating conditions.

5 Outlook

This thesis work demonstrates how the external environment can influence the properties of the complex stratum corneum membrane. Our systematic investigations of how hydration affects the macroscopic properties of the skin barrier increase the understanding of, for example, what conditions that are required to make use of the skin occlusion effect for transdermal drug delivery. By employing techniques that provide molecular scale information on the structure and dynamics of the SC components we increase the understanding of, for example, why the permeability is elevated at higher SC hydration. We show how small polar molecules, like glycerol and urea, affect the stratum corneum properties and how these molecules can be used to regulate the permeability with respect to the external water activity. These findings form a framework of knowledge that can be useful for future design optimization of transdermal delivery applications, as well as topical treatment of common deficient skin conditions, like dry skin.

Our approach to deal with the inherent complexity of the biological SC membrane was to use a simple system with well-defined boundary conditions in terms of the water activity, which is analogous to the osmotic stress technique (152). This approach has a clear advantage of that total focus of the influence of variations in the water activity on the SC properties is obtained, whereas distraction from other parameters is minimized. By combining this simple methodology with techniques that provide molecular scale information we gained a deeper understanding of the interplay between macroscopic and molecular properties and how these are influenced by the external water activity. This approach could turn out to be useful for other complex biological barrier systems where one can imagine hydration induced phase transitions to occur. Examples of this can be cuticle wax films on plants (153, 154), the lipid tear film formed on eyes (155, 156), and the molecularly ordered films, spontaneously formed at the air-liquid interface on solutions composed of, e.g., surfactants, polymers, or lipids (157, 158).

The ^{13}C PT ssNMR methodology developed by Nowacka and Topgaard (106, 107) provides unique information of the SC molecular components as shown in paper II, III, and V. A great benefit is that the method is particularly sensitive to the fluid components, which in general represent a minor fraction of the SC material. A future prospect is to examine the molecular properties of SC linked to various skin diseases and explore how deficient SC responds to hydration,

temperature, etc. The crusade of exploring the influence of common molecules employed in the field of skin cosmetics or various penetration enhancers employed in the transdermal research community are other options to explore.

The isothermal calorimetric method developed in paper VI, and used to determine the water activity in paper IV, is promising for various colloidal systems in the high water activity range due to its high flexibility in terms of sample composition and phase properties (i.e. solid or liquid samples). In addition, it would be possible to derive more detailed thermal information from the calorimeters used to humidify the N_2 gas before the gas reaches the actual measuring cell. In this respect, the method can be envisaged as a combination of the DVS and the isothermal sorption calorimeter and, with further optimization, this would be an interesting option to develop.

6 Acknowledgements

I have received support and assistance from many helpful people during the course of my thesis work.

First of all, I would like to acknowledge my supervisors **Emma, Johan, and Krister** for always being encouraging, generous with your time, and for guiding me throughout this work. The combination of your skills and ways of approaching various scientific problems has been of great value for the progress of my work and my knowledge. I also appreciate your sharing of contacts and all the opportunities that you have created for me. It has been a true pleasure to work together with you!

Many thanks to my co-authors…

Lars! I really enjoyed working with you. Thanks for all your friendly help, for always sharing knowledge, and being generous with your time. **Taut** for teaching me about impedance spectroscopy, your great support, and always finding time to discuss my questions. **Agnieszka** and **Daniel** for generously sharing your time and knowledge; I am truly glad for our collaborations! **Joke, Jenny**, **Dat**, and **Ihab** for your enthusiasm and good collaborations.

I would like to thank **Karin** for involving me as a teaching assistant and offering me a summer job at Physical Chemistry, where I finally ended up carrying on with my PhD studies. Thanks also to all friendly present and former colleagues at Physical Chemistry for creating a nice working atmosphere and keeping your doors open for discussions and questions.

All the friendly people in the "Biofilms group" for making my time as a guest at Malmö University so enjoyable!

I am grateful for all the help with technical and administrative issues that I have received from **Ingegerd**, **Lennart**, **Majlis**, **Ingrid**, **Christopher**, and **Maria** at Physical Chemistry. I would also like to thank B**engt** and **Stefan** at Building Materials for technical assistance and for being welcoming.

In the final stage of preparing my thesis, several people have been supportive and helpful to me. In particular, I am grateful to **Emma**, **Johan**, **Krister**, **Lars**, **Daniel**, **Taut**, and **Cathrine** for valuable comments on the thesis summary. **Hampus** for providing nice photographs with limited time and rather obscure instructions from me! **Paula** for all your help with editing and printing my thesis.

Fatima, **Juni**, and **Max**, thanks for always being by my side. You are the best!

7 References

1. Walpole, S. C., D. Prieto-Merino, P. Edwards, J. Cleland, G. Stevens, and I. Roberts. 2012. The weight of nations: An estimation of adult human biomass. Bmc Public Health 12.
2. Noe, D. A. 1991. A body-surface area nomogram based on the formula of Gehan and George. J Pharm Sci 80:501-501.
3. Kupper, T. S., and R. C. Fuhlbrigge. 2004. Immune surveillance in the skin: Mechanisms and clinical consequences. Nat Rev Immunol 4:211-222.
4. Schaefer, H., and T. E. Redelmeier. 1996. Structure and dynamics of the skin barrier, pp 1-42. In Skin barrier: Principles of percutaneous absorption. Karger.
5. Scheuplein, R. J., and I. H. Blank. 1971. Permeability of skin. Physiol Rev 51:702-747.
6. Lavker, R. M., and T. T. Sun. 1982. Heterogeneity in epidermal basal keratinocytes - Morphological and functional correlations. Science 215:1239-1241.
7. Candi, E., R. Schmidt, and G. Melino. 2005. The cornified envelope: A model of cell death in the skin. Nat Rev Mol Cell Bio 6:328-340.
8. Forslind, B., and M. Lindberg. 2004. Structure and function of the skin barrier: An introduction, pp 11-23. In Skin, hair, and nails Structure and function. B. Forslind, and M. Lindberg, editors. Marcel Dekker Inc.
9. Michaels, A. S., S. K. Chandrasekaran, and J. E. Shaw. 1975. Drug permeation through human skin. Theory and in vitro experimental measurement. AIChE J 21:985-996.
10. Elias, P. M. 1983. Epidermal lipids, barrier function, and desquamation. J Invest Dermatol Suppl 80:44-49.
11. Wertz, P., and L. Norlén. 2004. "Confidence intervals" for the "true" lipid compositions of the human skin barrier?, pp 85-106. In Skin, hair, and nails Structure and function. B. Forslind, and M. Lindberg, editors. Marcel Dekker Inc.
12. Motta, S., M. Monti, S. Sesana, R. Caputo, S. Carelli, and R. Ghidoni. 1993. Ceramide composition of the psoriatic scale. Biochim Biophys Acta 1182:147-151.
13. Lazo, N. D., J. G. Meine, and D. T. Downing. 1995. Lipids are covalently attached to rigid corneocyte protein envelopes existing predominantly as beta-sheets - A solid-state nuclear magnetic resonance study. J Invest Dermatol 105:296-300.
14. Wertz, P. W., and D. T. Downing. 1987. Covalently bound omega-hydroxyacylsphingosine in the stratum corneum. Biochim Biophys Acta 917:108-111.

15. Wertz, P. W., D. C. Swartzendruber, D. J. Kitko, K. C. Madison, and D. T. Downing. 1989. The role of the corneocyte lipid envelopes in cohesion of the stratum corneum. J Invest Dermatol 93:169-172.
16. Behne, M., Y. Uchida, T. Seki, P. O. de Montellano, P. M. Elias, and W. M. Holleran. 2000. Omega-hydroxyceramides are required for corneocyte lipid envelope (CLE) formation and normal epidermal permeability barrier function. J Invest Dermatol 114:185-192.
17. Wertz, P. W., and D. T. Downing. 1983. Ceramides of pig epidermis - Structure determination. J Lipid Res 24:759-765.
18. Schaefer, H., and T. E. Redelmeier. 1996. Composition and structure of the stratum corneum, pp 43-86. In Skin barrier: Principles of percutaneous absorption. Karger.
19. Singer, S. J., and G. L. Nicolson. 1972. Fluid mosaic model of structure of cell membranes. Science 175:720-&.
20. Boncheva, M., F. Damien, and V. Normand. 2008. Molecular organization of the lipid matrix in intact stratum corneum using ATR-FTIR spectroscopy. BBA-Biomembranes 1778:1344-1355.
21. Bouwstra, J. A., G. S. Gooris, M. A. Salomons-De Vries, J. A. van der Spek, and W. Bras. 1992. Structure of human stratum corneum as a function of temperature and hydration: A wide-angle X-ray diffraction study. Int J Pharm 84:205-216.
22. Bouwstra, J. A., G. S. Gooris, J. A. van der Spek, and W. Bras. 1991. Structural investigations of human stratum corneum by small-angle X-ray scattering. J Invest Dermatol 97:1005-1012.
23. Garson, J. C., J. Doucet, J. L. Leveque, and G. Tsoucaris. 1991. Oriented structure in human stratum corneum revealed by X-ray-diffraction. J Invest Dermatol 96:43-49.
24. Gay, C. L., R. H. Guy, G. M. Golden, V. H. Mak, and M. L. Francoeur. 1994. Characterization of low-temperature (i.e., < 65 degrees C) lipid transitions in human stratum corneum. J Invest Dermatol 103:233-239.
25. Hatta, I., N. Ohta, K. Inoue, and N. Yagi. 2006. Coexistence of two domains in intercellular lipid matrix of stratum corneum. BBA-Biomembranes 1758:1830-1836.
26. Silva, C., D. Topgaard, V. Kocherbitov, S. JJS, A. Pais, and E. Sparr. 2007. Stratum corneum hydration: phase transformations and mobility in stratum corneum, extracted lipids and isolated corneocytes. Biochim Biophys Acta 1768:2647-2659.
27. White, S. H., D. Mirejovsky, and G. I. King. 1988. Structure of lamellar lipid domains and corneocyte envelopes of murine stratum corneum. An x-ray diffraction study. Biochemistry 27:3725-3732.
28. Iwai, I., H. Han, L. d. Hollander, S. Svensson, L.-G. Ofverstedt, J. Anwar, J. Brewer, M. Bloksgaard, A. Laloeuf, D. Nosek, S. Masich, L. A. Bagatolli, U. Skoglund, and L. Norlen. 2012. The human skin barrier is organized as stacked bilayers of fully extended ceramides with cholesterol molecules associated with the ceramide sphingoid moiety. J Invest Dermatol 132:2215-2225.
29. Bouwstra, J. A., F. E. R. Dubbelaar, G. S. Gooris, and M. Ponec. 2000. The lipid organisation in the skin barrier. Acta Derm Venereol 208:23-30.

30. Forslind, B. 1994. A domain mosaic model of the skin barrier. Acta Derm Venereol 74:1-6.
31. Hill, J. R., and P. W. Wertz. 2003. Molecular models of the intercellular lipid lamellae from epidermal stratum corneum. BBA-Biomembranes 1616:121-126.
32. Bouwstra, J. A., G. S. Gooris, W. Bras, and D. T. Downing. 1995. Lipid organization in pig stratum corneum. J Lipid Res 36:685-695.
33. Fuchs, E., and D. W. Cleveland. 1998. A structural scaffolding of intermediate filaments in health and disease. Science 279:514-519.
34. Steinert, P. M. 1993. Structure, function, and dynamics of keratin intermediate filaments. J Invest Dermatol 100:729-734.
35. Knorr, F., J. Lademann, A. Patzelt, W. Sterry, U. Blume-Peytavi, and A. Vogt. 2009. Follicular transport route - Research progress and future perspectives. Eur J Pharm Biopharm 71:173-180.
36. Bodde, H. E., I. Van den Brink, H. K. Koerten, and F. H. N. De Haan. 1991. Visualization of in vitro percutaneous penetration of mercuric chloride; transport through intercellular space versus cellular uptake through desmosomes. J Control Release 15:227-236.
37. Johnson, M. E., D. Blankschtein, and R. Langer. 1997. Evaluation of solute permeation through the stratum corneum: Lateral bilayer diffusion as the primary transport mechanism. J Pharm Sci 86:1162-1172.
38. Potts, R., and M. Francoeur. 1990. Lipid biophysics of water loss through the skin. Proc Natl Acad Sci USA 87:3871-3873.
39. Potts, R. O., and R. H. Guy. 1992. Predicting skin permeability. Pharm Res 9:663-669.
40. Albery, W. J., and J. Hadgraft. 1979. Percutaneous absorption - In vivo experiments. J Pharm Pharmacol 31:140-147.
41. Naik A, K., YN, Guy RH. 2000. Transdermal drug delivery: overcoming the skin's barrier function. Pharm Sci Technol To 3:318-326.
42. Prausnitz, M. R., and R. Langer. 2008. Transdermal drug delivery. Nat Biotechnol 26:1261-1268.
43. Kalia, Y. N., A. Naik, J. Garrison, and R. H. Guy. 2004. Iontophoretic drug delivery. Adv Drug Deliv Rev 56:619-658.
44. Prausnitz, M. R., V. G. Bose, R. Langer, and J. C. Weaver. 1993. Electroporation of mammalian skin - A mechanism to enhance transdermal drug delivery. P Natl Acad Sci USA 90:10504-10508.
45. Henry, S., D. V. McAllister, M. G. Allen, and M. R. Prausnitz. 1998. Microfabricated microneedles: A novel approach to transdermal drug delivery. J Pharm Sci 87:922-925.
46. Mitragotri, S., D. Blankschtein, and R. Langer. 1995. Ultrasound-mediated transdermal protein delivery. Science 269:850-853.
47. Williams, A. C., and B. W. Barry. 2004. Penetration enhancers. Adv Drug Deliv Rev 56:603-618.
48. Subedi, R. K., S. Y. Oh, M.-K. Chun, and H.-K. Choi. 2010. Recent advances in transdermal drug delivery. Arch Pharm Res 33:339-351.

49. Zhang, Q., J. E. Grice, P. Li, O. G. Jepps, G.-J. Wang, and M. S. Roberts. 2009. Skin solubility determines maximum transepidermal flux for similar size molecules. Pharm Res 26:1974-1985.
50. Kasprzyk-Hordern, B., R. M. Dinsdale, and A. J. Guwy. 2007. Multi-residue method for the determination of basic/neutral pharmaceuticals and illicit drugs in surface water by solid-phase extraction and ultra performance liquid chromatography-positive electrospray ionisation tandem mass spectrometry. J Chromatogr 1161:132-145.
51. Chapman, S. J., and A. Walsh. 1990. Desmosomes, corneosomes and desquamation - An ultrastructural-study of adult-pig epidermis. Arch Dermatol Res 282:304-310.
52. Bonte, F., A. Saunois, P. Pinguet, and A. Meybeck. 1997. Existence of a lipid gradient in the upper stratum corneum and its possible biological significance. Arch Dermatol Res 289:78-82.
53. Weerheim, A., and M. Ponec. 2001. Determination of stratum corneum lipid profile by tape stripping in combination with high-performance thin-layer chromatography. Arch Dermatol Res 293:191-199.
54. Cox, P., and C. A. Squier. 1986. Variations in lipids in different layers of porcine epidermis. J Invest Dermatol 87:741-744.
55. Ranasinghe, A. W., P. W. Wertz, D. T. Downing, and I. C. Mackenzie. 1986. Lipid composition of cohesive and desquamated corneocytes from mouse ear skin. J Invest Dermatol 86:187-190.
56. Bouwstra, J. A., G. S. Gooris, F. E. R. Dubbelaar, and M. Ponec. 1999. Cholesterol sulfate and calcium affect stratum corneum lipid organization over a wide temperature range. J Lipid Res 40:2303-2312.
57. Forslind, B., Y. Werner-Linde, M. Lindberg, and J. Pallon. 1999. Elemental analysis mirrors epidermal differentiation. Acta Derm Venereol 79:12-17.
58. Öhman, H., and A. Vahlquist. 1994. In vivo studies concerning a ph gradient in human stratum corneum and upper epidermis. Acta Derm Venereol 74:375-379.
59. Brattsand, M., K. Stefansson, C. Lundh, Y. Haasum, and T. Egelrud. 2005. A proteolytic cascade of kallikreins in the stratum corneum. J Invest Dermatol 124:198-203.
60. Lee, S. H., P. M. Elias, E. Proksch, G. K. Menon, M. Q. Man, and K. R. Feingold. 1992. Calcium and potassium are important regulators of barrier homeostasis in murine epidermis. J Clin Invest 89:530-538.
61. Caspers, P. J., G. W. Lucassen, H. A. Bruining, and G. J. Puppels. 2000. Automated depth-scanning confocal Raman microspectrometer for rapid in vivo determination of water concentration profiles in human skin. J Raman Spectrosc 31:813-818.
62. Warner, R. R., M. C. Myers, and D. A. Taylor. 1988. Electron probe analysis of human skin: Determination of the water concentration profile. J Invest Dermatol 90:218-224.
63. Blank, I. H. 1953. Further observations on factors which influence the water content of the stratum corneum. J Invest Dermatol 21:259-271.
64. Katagiri, C., J. Sato, J. Nomura, and M. Denda. 2003. Changes in environmental humidity affect the water-holding property of the stratum

corneum and its free amino acid content, and the expression of filaggrin in the epidermis of hairless mice. J Dermatol Sci 31:29-35.
65. Scott, I. R., and C. R. Harding. 1986. Filaggrin breakdown to water binding-compounds during development of the rat stratum-corneum is controlled by the water activity of the environment. Dev Biol 115:84-92.
66. Harding, C. R., A. Watkinson, A. V. Rawlings, and I. R. Scott. 2000. Dry skin, moisturization and corneodesmolysis. Int J Cosmet Sci 22:21-52.
67. Watkinson, A., C. Harding, A. Moore, and P. Coan. 2001. Water modulation of stratum corneum chymotryptic enzyme activity and desquamation. Arch Dermatol Res 293:470-476.
68. Caspers, P. J., G. W. Lucassen, E. A. Carter, H. A. Bruining, and G. J. Puppels. 2001. In vivo confocal Raman microspectroscopy of the skin: Noninvasive determination of molecular concentration profiles. J Invest Dermatol 116:434-442.
69. Barrett, J. G., and I. R. Scott. 1983. Pyrrolidone carboxylic-acid synthesis in guinea-pig epidermis. J Invest Dermatol 81:122-124.
70. Scott, I. R. 1981. Factors controlling the expressed activity of histidine ammonia-lyase in the epidermis and the resulting accumulation of urocanic acid. Biochem J 194:829-838.
71. Choi, E. H., M. Q. Man, F. S. Wang, X. J. Zhang, B. E. Brown, K. R. Feingold, and P. M. Elias. 2005. Is endogenous glycerol a determinant of stratum corneum hydration in humans? Journal of Investigative Dermatology 125:288-293.
72. Yancey, P. H., M. E. Clark, S. C. Hand, R. D. Bowlus, and G. N. Somero. 1982. Living with water-stress - Evolution of osmolyte systems. Science 217:1214-1222.
73. Yancey, P. H. 2005. Organic osmolytes as compatible, metabolic and counteracting cytoprotectants in high osmolarity and other stresses. J Exp Biol 208:2819-2830.
74. Loden, M. 2003. Role of topical emollients and moisturizers in the treatment of dry skin barrier disorders. Am J Clin Dermatol 4:771-788.
75. Sybert, V. P., B. A. Dale, and K. A. Holbrook. 1985. Ichthyosis vulgaris - Identification of a defect in synthesis of filaggrin correlated with an absence of keratohyaline granules. J Invest Dermatol 84:191-194.
76. Sandilands, A., C. Sutherland, A. D. Irvine, and W. H. I. McLean. 2009. Filaggrin in the frontline: Role in skin barrier function and disease. J Cell Sci 122:1285-1294.
77. Hikima, T., and H. Maibach. 2006. Skin penetration flux and lag-time of steroids across hydrated and dehydrated human skin in vitro. Biol Pharm Bull 29:2270-2273.
78. Zhai, H., and I. Maibach Howard. 2002. Occlusion vs. skin barrier function. Skin Res Technol 8:1-6.
79. Alonso, A., N. Meirelles, V. Yushmanov, and M. Tabak. 1996. Water increases the fluidity of intercellular membranes of stratum corneum: Correlation with water permeability, elastic, and electric resistance properties. J Invest Dermatol 106:1058-1063.

80. Blank, I., J. Moloney, A. Emslie, I. Simon, and C. Apt. 1984. The diffusion of water across the stratum corneum as a function of its water content. J Invest Dermatol 82:182-194.
81. Nakazawa, H., N. Ohta, and I. Hatta. 2012. A possible regulation mechanism of water content in human stratum corneum via intercellular lipid matrix. Chem Phys Lipids 165:238-243.
82. Ohta, N., S. Ban, H. Tanaka, S. Nakata, and I. Hatta. 2003. Swelling of intercellular lipid lamellar structure with short repeat distance in hairless mouse stratum corneum as studied by X-ray diffraction. Chem Phys Lipids 123:1-8.
83. Costa-Balogh, F. O., H. Wennerström, L. Wadsö, and E. Sparr. 2006. How small polar molecules protect membrane systems against osmotic stress: The urea-water-phospholipid system. J Phys Chem B 110:23845-23852.
84. Nowacka, A., S. Douezan, L. Wadso, D. Topgaard, and E. Sparr. 2012. Small polar molecules like glycerol and urea can preserve the fluidity of lipid bilayers under dry conditions. Soft Matter 8:1482-1491.
85. Jacobi, U., M. Kaiser, R. Toll, S. Mangelsdorf, H. Audring, N. Otberg, W. Sterry, and J. Lademann. 2007. Porcine ear skin: an in vitro model for human skin. Skin Res Technol 13:19-24.
86. Bronaugh, R. L., R. F. Stewart, and E. R. Congdon. 1982. Methods for in vitro percutaneous absorption studies. 2. Animal models for human skin. Toxicol Appl Pharm 62:481-488.
87. Dick, I. P., and R. C. Scott. 1992. Pig ear skin as an in vitro model for human skin permeability. J Pharm Pharmacol 44:640-645.
88. Reifenrath, W. G., E. M. Chellquist, E. A. Shipwash, and W. W. Jederberg. 1984. Evaluation of animal models for predicting skin penetration in man. Fund Appl Toxicol 4:S224-S230.
89. Vallet, V., C. Cruz, D. Josse, A. Bazire, G. Lallement, and I. Boudry. 2007. In vitro percutaneous penetration of organophosphorus compounds using full-thickness and split-thickness pig and human skin. Toxicol in Vitro 21:1182-1190.
90. Sekkat, N., Y. N. Kalia, and R. H. Guy. 2002. Biophysical study of porcine ear skin in vitro and its comparison to human skin in vivo. J Pharm Sci 91:2376-2381.
91. Marro, D., R. H. Guy, and M. B. Delgado-Charro. 2001. Characterization of the iontophoretic permselectivity properties of human and pig skin. J Controlled Release 70:213-217.
92. Yamamoto, T., and Y. Yamamoto. 1976. Electrical properties of the epidermal stratum corneum. Med Biol Eng 14:151-158.
93. Kalia, Y. N., F. Pirot, and R. H. Guy. 1996. Homogeneous transport in a heterogeneous membrane: water diffusion across human stratum corneum in vivo. Biophys J 71:2692-2700.
94. Clar, E. J., C. P. Her, and C. G. Sturelle. 1975. Skin impedance and moisturization. J Soc Cosmet Chem 26:337-353.
95. Jequier, E., and F. Constant. 2010. Water as an essential nutrient: the physiological basis of hydration. Eur J Clin Nutr 64:115-123.

96. Schmidt, E., and U. Grigull. 1982. Properties of water and steam in SI-units: 0-800 deg. Celcius, 0-1000 bar. Springer-Verlag.
97. Verevkin, S. P. 2005. Phase changes in pure component systems: Liquids and gases. In Experimental thermodynamics, pp 5-30. R. D. Weir, and T. W. D. Loos, editors. Elsevier.
98. Berling, D., D. Hallen, T. H. Lilly, and G. Olofsson. 1997. Solvent activity meter based on a high sensitivity heat-flow microcalorimeter. Thermochim Acta 298:3-7.
99. Berling, D., B. Jönsson, and G. Olofsson. 1999. The use of isothermal heat-conduction calorimetry in direct measurements of solvent vapour pressure. J Solution Chem 28:693-710.
100. Scatchard, G., W. J. Hamer, and S. E. Wood. 1938. Isotonic solutions I. The chemical potential of water in aqueous solutions of sodium chloride, potassium chloride, sulfuric acid, sucrose, urea and glycerol at 25 deg. C. J Am Chem Soc 60:3061-3070.
101. Jakasa, I., M. M. Verberk, A. L. Bunge, J. Kruse, and S. Kezic. 2006. Increased permeability for polyethylene glycols through skin compromised by sodium lauryl sulfate. Exp Dermatol 15:801-807.
102. Tsai, J., P. Hung, and H. Sheu. 2001. Molecular weight dependence of polyethylene glycol penetration across acetone-disrupted permeability barrier. Arch Dermatol Res 293:302-307.
103. Tsai, J., L. Shen, H. Sheu, and C. LU. 2003. Tape stripping and sodium dodecyl sulfate treatment increase the molecular weight cutoff of polyethylene glycol penetration across murine skin. Arch Dermatol Res 295:169-174.
104. Albèr C., Brandner B., Björklund S., Billsten P., Corkery R., and E. J. 2013. Effects of water gradients and use of urea on skin ultrastructure evaluated by confocal Raman microspectroscopy. Submitted to BBA-Biomembranes.
105. Evans, D. F., and H. Wennerström. 1999. Solutes and solvents, self-assembly of amphiphiles, pp 295-350. In The colloidal domain - where physics, chemistry, biology and technology meet, 2nd ed. Wiley-VCH, New York.
106. Nowacka, A., N. Bongartz, O. H. S. Ollila, T. Nylander, and D. Topgaard. 2013. Signal intensities in 1H-13C CP and INEPT MAS NMR of liquid crystals. J Magn Reson 230:165-175.
107. Nowacka, A., P. C. Mohr, J. Norrman, R. W. Martin, and D. Topgaard. 2010. Polarization transfer solid-state NMR for studying surfactant phase behavior. Langmuir 26:16848-16856.
108. Schaefer, J., E. O. Stejskal, and R. Buchdahl. 1975. High-resolution carbon-13 nuclear magnetic resonance study of some solid, glassy polymers. Macromolecules 8:291-296.
109. Morris, G. A., and R. Freeman. 1979. Enhancement of nuclear magnetic resonance signals by polarization transfer. J Am Chem Soc 101:760-762.
110. Pines, A., J. S. Waugh, and M. G. Gibby. 1972. Proton enhanced nuclear induction spectroscopy - Method for high-resolution NMR of dilute spins in solids. J Chem Phys 56:1776-1777.
111. Kalia, Y. N., and R. H. Guy. 1995. The electrical characteristics of human skin in vivo. Pharm Res 12:1605-1613.

112. Oh, S. Y., L. Leung, D. Bommannan, R. H. Guy, and R. O. Potts. 1993. Effect of current, ionic strength and temperature on the electrical properties of skin. J Control Release 27:115-125.
113. DeNuzzio, J. D., and B. Berner. 1990. Electrochemical and iontophoretic studies of human skin. J Control Release 11:105-112.
114. Kontturi, K., and L. Murtomaki. 1994. Impedance spectroscopy in human skin. A refined model. Pharm Res 11:1355-1357.
115. Hirschorn, B., M. E. Orazem, B. Tribollet, V. Vivier, I. Frateur, and M. Musiani. 2010. Determination of effective capacitance and film thickness from constant-phase-element parameters. Electrochim Acta 55:6218-6227.
116. Brug, G. J., A. L. G. Vandeneeden, M. Sluytersrehbach, and J. H. Sluyters. 1984. The analysis of electrode impedances complicated by the presence of a constant phase element. J Electroanal Chem 176:275-295.
117. Cole, K. S. 1968. Membranes, ions, and impulses. University of California Press, Berkeley.
118. Orazem, M. E., N. Pebere, and B. Tribollet. 2006. Enhanced graphical representation of electrochemical impedance data. J Electrochem Soc 153:B129-B136.
119. Bouwstra, A. J., G. Gooris, and S. H. White. 1997. X-ray analysis of the stratum corneum and its lipids, pp 41-85. In Mechanisms of transdermal drug delivery. R. O. Potts, and R. H. Guy, editors. Marcel Dekker.
120. Labrador, A., Y. Cerenius, K. Theodor, C. Svenssson, J. Nygaard, and T. Plivelic. 2012. The yellow SAXS mini-hutch at MAX IV laboratory. 11th International Conference on Synchrotron Radiation Instrumentation, Lyon, France, 9-13 July.
121. Wadso, L., and N. Markova. 2000. A double twin isothermal microcalorimeter. Thermochim Acta 360:101-107.
122. Wadsö, I., and L. Wadsö. 1996. A new method for determination of vapour sorption isotherms using a twin double microcalorimeter. Thermochim Acta 271:179-187.
123. Sparr, E., and H. Wennerström. 2001. Responding phospholipid membranes-interplay between hydration and permeability. Biophys J 81:1014-1028.
124. Zhai, H., J. P. Ebel, R. Chatterjee, K. J. Stone, V. Gartstein, K. D. Juhlin, A. Pelosi, and H. I. Maibach. 2002. Hydration vs. skin permeability to nicotinates in man. Skin Res Technol 8:13-18.
125. Peck, K. D., A. H. Ghanem, and W. I. Higuchi. 1995. The effect of temperature upon the permeation of polar and ionic solutes through human epidermal membrane. J Pharm Sci 84:975-982.
126. Sims, S. M., W. I. Higuchi, and V. Srinivasan. 1991. Skin alteration and convective solvent flow effects during iontophoresis: I. Neutral solute transport across human skin. Int J Pharm 69:109-121.
127. Karande, P., A. Jain, and S. Mitragotri. 2006. Relationships between skin's electrical impedance and permeability in the presence of chemical enhancers. J Control Release 110:307-313.
128. Nishikawa, N., Y. Tanizawa, S. Tanaka, Y. Horiguchi, H. Matsuno, and T. Asakura. 1998. pH dependence of the coiled-coil structure of keratin

intermediate filament in human hair by C-13 NMR spectroscopy and the mechanism of its disruption. Polym J 30:125-132.
129. Yoshimizu, H., and I. Ando. 1990. Conformational characterization of wool keratin and S-(carboxymethyl)kerateine in the solid-state by C-13 CP/MAS NMR-spectroscopy. Macromolecules 23:2908-2912.
130. Bengsch, E., B. Perly, C. Deleuze, and A. Valero. 1986. A general rule for the assignment of the carbon-13 NMR peaks in fatty acid chains. J Magn Reson 68:1-13.
131. Soubias, O., F. Jolibois, V. Reat, and A. Milon. 2004. Understanding sterol-membrane interactions. Part II: Complete H-1 and C-13 assignments by solid-state NMR spectroscopy and determination of the hydrogen-bonding partners of cholesterol in a lipid bilayer. Chem-Eur J 10:6005-6014.
132. Kisic, A., M. Tsuda, R. J. Kulmacz, W. K. Wilson, and G. J. Schroepfer Jr. 1995. Sphingolipid bases. A revisitation of the O-methyl derivatives of sphingosine. Isolation and characterization of diacetate derivatives, with revised 13C nuclear magnetic resonance assignments for D-erythro-sphingosine. J Lipid Res 36:787-805.
133. Earl, W. L., and D. L. VanderHart. 1979. Observations in solid polyethylenes by carbon-13 magnetic resonance with magic angle sample spinning. Macromolecules 12:762-767.
134. Akomeah, F., T. Nazir, G. P. Martin, and M. B. Brown. 2004. Effect of heat on the percutaneous absorption and skin retention of three model penetrants. Eur J Pharm Sci 21:337-345.
135. Blank, I. H., R. J. Scheuplein, and Macfarla.Dj. 1967. Mechanism of percutaneous absorption. 3. Effect of temperature on transport of non-electrolytes across skin. J Invest Dermatol 49:582-589.
136. Ghadially, R., J. T. Reed, and P. M. Elias. 1996. Stratum corneum structure and function correlates with phenotype in psoriasis. J Invest Dermatol 107:558–564.
137. Loden, M., H. Olsson, T. Axell, and Y. W. Linde. 1992. Friction, capacitance and transepidermal water-loss (TEWL) in dry atopic and normal skin. Brit J Derm 126:137-141.
138. Hey, M. J., D. J. Taylor, and W. Derbyshire. 1978. Water sorption by human callus. Biochim Biophys Acta 540:518-533.
139. Craven, B. M. 1976. Crystal structure of cholesterol monohydrate. Nature 260:727-729.
140. Hinsberg, W. H. M. C. v., J. C. Verhoef, H. E. Junginger, and H. E. Bodde. 1995. Thermoelectrical analysis of the human skin barrier. Thermochim Acta 248:303-318.
141. Norlén, L., E. Axelsson, and B. Forslind. 1997. Stratum corneum swelling. Biophysical and computer assisted quantitative assessments. Arch Dermatol Res 289:506–513.
142. Bouwstra, J., A. Graaff, G. Gooris, J. Nijsse, J. Wiechers, and A. Aelst. 2003. Water distribution and related morphology in human stratum corneum at different hydration levels. J Invest Dermatol 120:750-758.

143. Norlen, L., A. Emilson, and B. Forslind. 1997. Stratum corneum swelling. Biophysical and computer assisted quantitative assessments. Arch Dermatol Res 289:506-513.
144. Richter, T., C. Peuckert, M. Sattler, K. Koenig, I. Riemann, U. Hintze, K. P. Wittern, R. Wiesendanger, and R. Wepf. 2004. Dead but highly dynamic - The stratum corneum is divided into three hydration zones. Skin Pharmacol Physi 17:246-257.
145. Warner, R. R., Y. L. Boissy, N. A. Lilly, M. J. Spears, K. McKillop, and J. L. Marshall. 1999. Water disrupts stratum corneum lipid lamellae: damage is similar to surfactants J Invest Dermatol 113:960-966.
146. Warner, R. R., K. J. Stone, and Y. L. Boissy. 2003. Hydration disrupts human stratum corneum ultrastructure. J Invest Dermatol 120:275-284.
147. Grice, K., H. Sattar, and H. Baker. 1973. Urea and retinoic acid in ichthyosis and their effect on transepidermal water-loss and water holding capacity of stratum corneum. Acta Derm Venereol 53:114-118.
148. Bettinger, J., M. Gloor, A. Vollert, P. Kleesz, J. Fluhr, and W. Gehring. 1999. Comparison of different non-invasive test methods with respect to the effect of different moisturizers on skin. Skin Res Technol 5:21-27.
149. Loden, M., A. C. Andersson, C. Anderson, I. M. Bergbrant, T. Frodin, H. Ohman, M. H. Sandstrom, T. Sarnhult, E. Voog, B. Stenberg, E. Pawlik, A. Preisler-Haggqvist, A. Svensson, and M. Lindberg. 2002. A double-blind study comparing the effect of glycerin and urea on dry, eczematous skin in atopic patients. Acta Derm Venereol 82:45-47.
150. Froebe, C. L., F. A. Simion, H. Ohlmeyer, L. D. Rhein, J. Mattai, R. H. Cagan, and S. E. Friberg. 1990. Prevention of stratum corneum lipid phase transitions in vitro by glycerol - An alternative mechanism for skin moisturization. J Soc Cosmet Chem 41:51-65.
151. Blank, I. H. 1952. Factors which influence the water content of the stratum corneum. J Invest Dermatol 18:433-440.
152. LeNeveu, D. M., R. P. Rand, and V. A. Parsegian. 1976. Measurement of forces between lecithin bilayers. Nature 259:601-603.
153. Bargel, H., K. Koch, Z. Cerman, and C. Neinhuis. 2006. Structure-function relationships of the plant cuticle and cuticular waxes - A smart material? Funct Plant Biol 33:893-910.
154. Schreiber, L., K. Schorn, and T. Heimburg. 1997. H-2 NMR study of cuticular wax isolated from Hordeum vulgare L. leaves: identification of amorphous and crystalline wax phases. Eur Biophys J Biophy 26:371-380.
155. Butovich, I. A., T. J. Millar, and B. M. Ham. 2008. Understanding and analyzing meibomian lipids - A review. Curr Eye Res 33:405.
156. Leiske, D. L., C. E. Miller, L. Rosenfeld, C. Cerretani, A. Ayzner, B. Lin, M. Meron, M. Senchyna, H. A. Ketelson, D. Meadows, S. Srinivasan, L. Jones, C. J. Radke, M. F. Toney, and G. G. Fuller. 2012. Molecular structure of interfacial human meibum films. Langmuir 28:11858.
157. Cevc, G., W. Fenzl, and L. Sigl. 1990. Surface induced X-ray reflection visualization of membrane orientation and fusion into multibilayers. Science 249:1161-1163.

158. O'Driscoll, B. M. D., E. A. Nickels, and K. J. Edler. 2007. Formation of robust, free-standing nanostructured membranes from catanionic surfactant mixtures and hydrophilic polymers. Chem Comm:1068–1070.